

POLITECNICO MILANO 1863

DIPARTIMENTO DI SCIENZE E TECNOLOGIE AEROSPAZIALI

CORSO DI LAUREA MAGISTRALE IN INGEGNERIA AERONAUTICA

Preliminary design of a 20 MW wind turbine

Relatore: Prof. Croce Alessandro

Tesi di laurea di:

Fabio Bellini

Matr. 842154

Anno accademico 2016/2017

Acknowledgements

I want to reward all those who helped me in the realization of my Thesis. First of all, I would like to thank my thesis supervisor prof. A. Croce, and all the staff of *PoliWind* research unit at Politecnico di Milano for giving me the possibility to carry out this research project, and for their precious advice. A special thanks goes to my tutor L. Sartori, for his patience and full availability in covering my doubts and support me when in trouble.

I must express my profound gratitude to my parents, my brother and all my friends for providing me with unfailing support and continuous encouragement throughout my years of study and through the process of researching and writing this Thesis. This accomplishment would not have been possible without them.

Thank you all.

This work is partially supported by the EU FP7 INNWIND project.

Abstract

In the last years, the design of wind turbines has evolved more and more towards large machines, in order to maximize the harvested wind energy and reduce the costs. A common practice in this type of studies consists in starting from the definition of an aero-elastic turbine model derived by scaling an existing one by means of suitable scaling laws. Often, this results in an overestimation of the mass of the various sub-components of the turbine, which then encounter significant loads through their operating lifetime. Specific techniques for loads and mass reduction must be applied to these machines in order to target a sensible reduction of the cost of energy.

This work is focused on the definition of a structural model for a conceptual 20 MW wind turbine through a step-by-step parametric design process in which the best performance in terms of mass, loads, energy production and cost of energy are sought. The overall process is performed in a multi-disciplinary optimization framework that allows to consider all the relevant aspects of the design. Initially, the structural optimization of a tentative wind turbine rotor was performed. Then, a constrained optimization of the blade prebend was conducted, with relevant advantages in terms of mass reduction and improvement of the power production. Then, a passive control system for loads reduction was introduced, through the application of a certain amount of fiber rotation in the laminae of some composite blade elements: this led to further loads reduction in most of the turbine structural elements. At this point two different refinements have been explored: on one side an active control system was adopted to further reduce ultimate and fatigue loads, while on the other a parametric study on the rotor planar solidity was performed to improve the aero-structural performance of the turbine. In both cases, advantages in accordance with expectations were encountered.

Sommario

Nel corso degli ultimi anni, il progetto di turbine eoliche si è spinto verso macchine di dimensioni sempre maggiori, con lo scopo di incrementare l'energia estratta dal vento e ridurre i costi. È ormai una pratica comune in questo tipo di studi, partire dalla definizione di un modello aeroelastico della turbina derivato, mediante opportune leggi di scalatura, da quello di una turbina già esistente, di dimensioni e potenza nominale inferiori. Spesso tuttavia, il risultato è un modello eccessivamente pesante che sviluppa dei carichi rilevanti nelle varie situazioni in cui si trova ad operare. Tecniche che mirano a ridurre i carichi e la massa devono essere necessariamente adottate su queste macchine, per poter ambire ad una riduzione dei costi.

Questo lavoro è incentrato sulla realizzazione di un modello strutturale di una turbina da 20 MW, al quale successivamente si sono applicate varie tecnologie con lo scopo di verificare gli eventuali vantaggi in termini di riduzione di massa e carichi, incrementi di energia annua prodotta e riduzione del costo dell'energia. Tutto ciò, in un contesto di ottimizzazione multi-disciplinare che permette di tenere in considerazione tutti gli aspetti rilevanti del design. Inizialmente è stata effettuata l'ottimizzazione strutturale del rotore della turbina. Dopodiché, un'ottimizzazione vincolata della pre-curvatura della pala è stata effettuata, con rilevanti effetti benefici per quanto riguarda la riduzione di massa e l'incremento di energia prodotta. Tuttavia, i carichi agenti sulla struttura della turbina sono aumentati a causa della maggior deflessione della pala. Si è quindi introdotto un sistema di controllo passivo che consiste nella rotazione delle fibre dei materiali compositi, con importanti riduzioni di carichi su molti elementi strutturali della macchina. A questo punto sono state approcciate due strade differenti: da una parte si è introdotto un controllo attivo per ridurre ulteriormente i carichi ultimi e a fatica, mentre in parallelo si sono effettuati studi sulla solidità del rotore con l'obiettivo di incrementare la producibilità della turbina eolica. In entrambi i casi si sono riscontrati vantaggi in accordo con le aspettative.

Contents

List of Figures	xi
List of Tables	xv
1 Introduction	1
1.1 Motivations and goals	1
1.2 State of the art	4
2 Optimization problem	9
2.1 Overall optimizer architecture	10
2.1.1 Aerodynamic tool	12
2.1.2 Control design	13
2.1.3 Prebend design	15

2.1.4	Structural design	16
2.1.5	Objective function	18
2.2	Certification guidelines	19
3	Models	21
3.1	Reference 20 MW model	22
3.1.1	Blade description	23
3.1.2	Tower description	24
3.1.3	Control	27
3.2	Baseline 20 MW model	28
4	Optimization studies	37
4.1	Prebend	38
4.2	Spar caps fiber rotation	41
4.3	IPC	44
4.4	Planar solidity	47
4.5	Results	51
5	Conclusions	53
5.1	Future developments	54
A	Controller data	57
	Bibliography	61

List of Figures

1.1.1 Upscaling trend during the last few years.	3
2.1.1 Overall architecture of the multi-level combined design procedure.	10
2.1.2 Example of Cp-Lambda and trajectory regulation curves.	15
3.1.1 Reference 20 MW blade geometrical properties.	25
3.1.2 Reference 20 MW blade mass and stiffness properties.	26
3.1.3 Tower thickness and diameter distributions.	27
3.2.1 Baseline 20 MW blade planform.	29
3.2.2 Internal blade layout: sectional elements (a) and structural components (b). Note: leading edge LE; trailing edge TE; suction side SS; pressure side PS.	30
3.2.3 Turbulent power curve and power coefficient.	32

3.2.4 Thickness distributions and lamination sequence of the blade elements for the Baseline 20 MW.	33
3.2.5 Baseline 20 MW blade stiffness properties compared with the Reference 20 MW ones.	34
4.0.1 Optimization analyses process flow.	38
4.1.1 Prebend distributions and consequent variation of the blade-tower clearance.	39
4.1.2 Performance percentage variation with respect to the Baseline 20 MW model.	40
4.1.3 Key loads percentage variation with respect to the Baseline 20 MW model.	40
4.2.1 F-BTC blade coupling parameters.	41
4.2.2 Performance percentage variation with respect to the 4 m Prebend model.	42
4.2.3 Key loads percentage variation with respect to the Prebend 4 m model.	43
4.2.4 Suction side spar cap thickness (a) and blade root fatigue DELs (b) variations.	44
4.3.1 Time history of blade pitch angle with and without IPC during a 13 m/s operational condition. In the second case slightly faster and larger pitch movement are required in order to achieve the improved load reductions.	45
4.3.2 Key loads percentage variation with respect to the F-BTC 6° model.	46
4.3.3 Performance percentage variation with respect to the F-BTC 6° model.	46
4.4.1 Chord, twist and relative thickness distribution variations.	47
4.4.2 Rated conditions comparison.	48

4.4.3 Performance percentage variation with respect to the F-BTC 6° model.	49
4.4.4 Key loads percentage variation with respect to the F-BTC 6° model.	50

List of Tables

2.1	Design constraints considered for the blade.	17
2.2	Design load cases	20
3.1	Overall characteristics of the wind turbine.	22
3.2	Blade airfoils.	24
3.3	Blade material properties.	30
3.4	Structural design optimization sections of the blade.	31
3.5	Mass, AEP and CoE comparison between Baseline and Reference models.	31
3.6	Ultimate loads comparison between Reference 20 MW and Baseline 20 MW.	35
3.7	Fatigue DEL loads comparison between Reference 20 MW and Baseline 20 MW.	35

4.1	Mass, AEP and CoE comparison between Prebend solutions and Baseline 20 MW.	39
4.2	Mass, AEP and CoE comparison between F-BTC solutions and Prebend 4 m.	42
4.3	Mass, AEP and CoE comparison between IPC solution and F-BTC 6° model.	45
4.4	Mass, AEP and CoE comparison between Solidity solutions and F-BTC 6° model.	49
4.5	Solutions comparison	51
A.1	Settings of the DTU Controller.	58

CHAPTER 1

Introduction

1.1 Motivations and goals

Wind energy is one of the most promising renewable energy sources in terms of performance and costs and, together with solar and geothermic energy generation, it will be crucial for the future human energy demand.

Indeed, in the last years, there was a significant interest in the development of methodologies and technologies for the design of a new generation of wind turbines. In particular, integrated aero-servo-elastic design optimization is found to be the best approach among many others different methods. Such multi-disciplinary approaches allow to design lighter and more economic turbines, starting from standard configurations and integrating new developed features. In fact, interdisciplinary interactions among structure, aerodynamics, hydrodynamics and control, can be properly accounted for in this way. The ability to describe the dynamic behavior of a wind turbine through high-fidelity models is fundamental for the understanding of the performance of horizontal and vertical axis wind turbines (HAWTs, VAWTs), leading to a better awareness of the potential improvements which can be developed in order to reduce the cost of energy.

This approach also permits an accurate prediction of the fatigue and ultimate load

conditions, a precise study of the stability of the machine and the possibility to synthesize dedicated control laws directly within the simulation environment. All these aspects are fundamental in order to increase the efficiency of the turbine and for an effective loads reduction. Besides, all these considerations affect the economical and technical feasibility of the project significantly.

Others simplified design strategies, despite being less time consuming, imply the risk of overlooking important coupling effects. Similar drawbacks can emerge when the design is carried out in an over-simplified methodological framework, in which for example only some parameters of the wind turbine are considered, while others are kept frozen. For example, changing the rotor size of a machine without considering the re-design of the control laws can't be considered an efficient and recommended practice, as it generally results in lower-than-expected performance.

Additionally, the use of a constrained optimization-based approach to design wind turbine components allows to automatically fulfill essential design requirements, which typically account for ultimate and lifetime structural integrity, maximum allowable deflections and the avoidance of resonance phenomena among the various components of the wind turbine. This latter requirement is usually solved by means of a targeted placement of the natural frequencies of the coupled system. The implementation of such operational constraints, as well as considerations on aeroelastic instabilities, guarantee that a physically-meaningful solution is achieved at the end of the optimization loop.

Such considerations are especially true when the focus is on beyond-state-of-art wind turbines in which, due to the outstanding size of the rotors, these problems and mutual interfaces become more and more complex. In fact in this case more flexibility in the beam-like elements, and thus larger deformations, have to be considered: these can affect performance, determine the onset of aeroelastic instabilities and possibly result in higher loads that further amplify the displacements with respect to the desired reference condition.

In these years, this aspect has become more and more important, since the main trend is to continuously upscale the wind turbines with the aim of increasing the power production and decreasing the cost of energy, considering its entire life-cycle. The considerations that drive the evolution of the wind energy market in this way are many but, from a business perspective, the primary one is the economic viability. Any other factor considered with the aim to minimize the number of wind turbines required for the bulk generation of electricity can be in fact related to this requirement in some way. For example, maintenance, transportation and infrastructure are fundamental cost items that decrease when fewer larger machines are employed to generate the same installed capacity. Another important aspect is the lower occupied land area for the same installed energy capacity, that

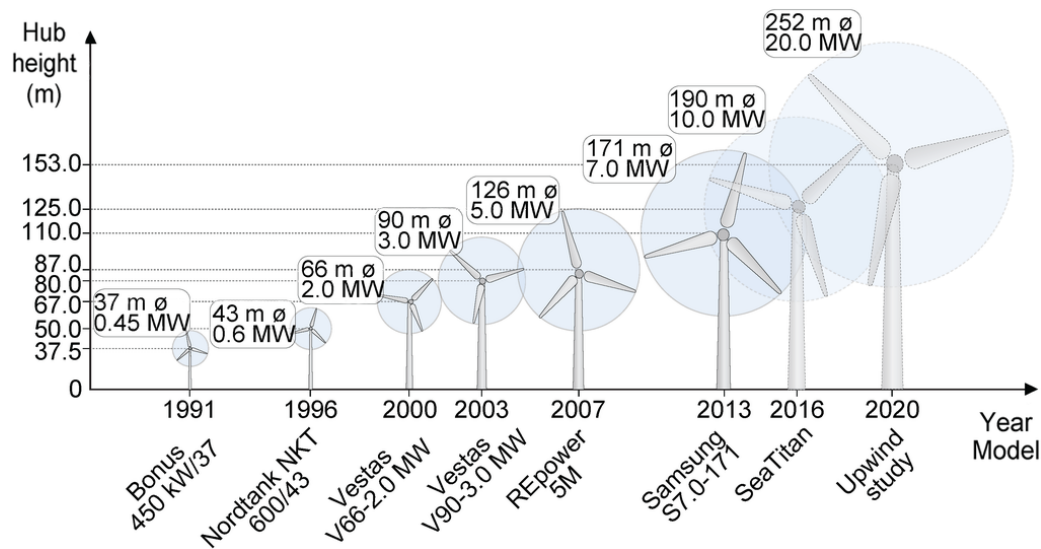


Figure 1.1.1: Upscaling trend during the last few years.

allows a higher energy harness from the same site, that is equivalent to a further cost reduction. This aspect is also tied to the fact that the available onshore areas for wind energy development are running out, especially in countries with a high population density or where possible wind sites do not match the standards for a profitable plant installation. Nowadays offshore wind energy offers the most attractive alternative considering that winds at the open sea are typically stronger and more stable than those inland, resulting in a significantly higher energy production. Additional advantages concern issues about noise and visual pollution, especially for the large scale.

The aim of this work is thus to link these two aspects of the modern wind turbine design approach. In particular it's focused on the preliminary design of a 20 MW wind turbine rotor, which follows the current dominant concept, i.e. a three-bladed, upwind, variable speed, pitch-regulated wind turbine. The purpose is to define a feasible and competitive solution, through the systematic use of a multi-disciplinary design approach.

This work is organized as follows: starting from a reference aero-elastic definition of the model (which is represented through lumped and distributed aero-structural characteristics) the first step was to obtain a feasible structural design which should ideally mimic the properties of the reference configuration. This step was achieved through the solution of a mass-minimizing optimization problem in which the main design variables were the thicknesses of individual structural components. Subsequently, this preliminary optimized solution was used as a starting point for parametric studies in which some design features were added or modified in order

to identify possible performance advantages. Particular attention was made, at this step, on passive and active control systems for loads mitigation, which can be considered a possible way to counteract the significant loads and massive structure derived by the upscaling method.

In this view, several optimization studies were performed by analyzing the impact of selected design features on the performance of the wind turbine. The studies affected the rotor solidity, the span-wise distribution of prebend, the introduction of Bending-Torsion Coupling induced by spar caps Fiber rotation (F-BTC) and the application of an Individual Pitch Controller (IPC) regulation strategy. The final optimal redesign was obtained as a combination of the configurations resulting from each individual parametric study, in order to combine the advantages coming from each design loop in a globally better wind turbine. Although the first design phase was focused on the mass and load reduction, a final study on the planar solidity of the rotor was carried out with the aim to improve the aerodynamic efficiency of the turbine, and thus the annual energy production.

Improvements could be made in future works in order to further reduce mass, loads and achieve a better cost of energy by either involving additional passive/active control systems or by conducting a fully-automated redesign process instead of the step-by-step performance enhancement methodology pursued in this work.

1.2 State of the art

Modern wind turbines are characterized by large rotor sizes and by a power production in the range of several megawatts. Current practice when designing a larger rotor is to draw a tentative solution by up-scaling an existing one. Two different approaches are usually adopted to this scope:

- **Linear scaling laws:** this methods is based on an analytic description of the turbine properties and its main parameters with respect to the rotor diameter, and eventually other few global parameters. It can be done under the assumption that all geometrical parameters scale linearly with the radius with the exception of gearbox, generator, and electronics that usually follows other scaling trends. Furthermore the topological definition of the wind turbine must be the same (number of blades, airfoil families, upwind/downwind orientation, manufacturing process and materials).

Typically these methods start from the expected rated power. Then the new turbine radius is calculated after some theoretical considerations about

power production; thereafter the *scaling ratio* (SR) can be calculated as the ratio between the new (R_f) and the starting (R_i) rotors radius:

$$SR = \frac{R_f}{R_i} \quad (1.2.1)$$

Finally all relevant parameters (Q) for the final configuration, are computed by multiplying the parameters of the initial turbine by a power of SR ,

$$Q_f = Q_i * (SR)^{SF} \quad (1.2.2)$$

where SF is the *scaling factor*, which describes how the parameter is expected to scale. For instance, a volume property scales as R^3 and, therefore, its scaling factor is assumed to be 3.

This method is largely employed and documented in the literature. Among others, remarkable work in this field is proposed by Molly (1989) [33], Ashuri (2012) [2] and Jamieson (2011) [27], Nijssen et al. (2001) [36], Chaviaropoulos (2007) [15] or Ashuri and Zaaier (2008) [1].

Attempts with a non linear approach were also tried, like for example the upscaling technique presented by Capponi et al. (2011) [14], but the literature in this way is not very wide.

- **Using existing data:** consists in collecting the data from the largest possible set of wind turbines. This often results in a scattering of the data, that must be analyzed with some interpolation techniques in order to catch the desired scaling trends. This method is less common than the previous one, due to the fact that the data from industries are often confidential and not publicly available.

When larger-than-existing wind turbines have to be studied, a fundamental limit is that extrapolation techniques have to be used: this introduces large uncertainties in the design, which are much bigger as further the extrapolation goes outside the available data range.

The most comprehensive work in this context is carried out by Jamieson (2007) [28].

In both cases, the components that have to be examined with more attention are the blades, the low speed shaft and the tower, since they are characterized by a high flexibility and, at the same time, they are responsible for the transmission of the loads across the sub-components of the wind turbine.

Some other useful trends regarding for example loads, masses and costs, could also be extracted to investigate the scaling phenomenon more carefully, keeping in mind also the economically and feasibility aspects of the problem.

Generally, a trend identified from existing data can be more accurate than one from linear scaling laws, due to the complexity of the problem that can't be properly described by simple geometrical assumptions. In particular linear scaling laws often fail the prediction of the trend exponent for the component masses. Usually these are expected to scale with a cubic power of the radius ratio since they are related to volume, but the existing data result in a lower scaling factor for many components of the turbine. This effect is the result of technology developments that somehow attempt to counteract the principles of linear scaling laws.

Attention has to be made also for the loads scaling, because only stationary forces and bending moments can be treated with linear scaling models and often the trends correspond to a simple cubic scaling law; instead, the effective ultimate and fatigue design loads in existing data correspond to non-stationary loads, in most cases with scaling law exponents that tend to exceed the cubic power. This is a consequence of the high blade mass, that often introduces significant cyclic loads, especially in fore-aft and side-side components. An increasing effect of turbulence with scale may also contribute to the exponents being greater than cubic. On the other hand, the reduction in RPM, due to the constant tip speed assumption, will reduce the fatigue loading.

The aerodynamic performance prediction is expected to follow a "square" power of the scaling ratio, and this represents a valid predictive value in most cases. This means that the rotor area is a good measure for the prediction of the captured energy by the scaled wind turbine. This fact is valid especially for a classical control strategy in which the rated power is achieved following up the ideal maximum aerodynamic efficiency, known as the Betz limit, or in other words performing the energy capture at an axial induction factor of $1/3$ up to the rated condition. Many other effects that can affect both power and loads have not often been included in the theoretical upscaling laws. Those effects can be of lesser or greater importance as they account for the change in Reynolds number related to the boundary layer effects, greater influence of wind shear effects due to the higher turbine high-rise, non-linearities due to large deflections, increased risk of buckling failure modes, etc.

All these considerations show how technology breakthroughs in designing lighter machines are prerequisites for further upscaling in a cost-efficient way, since the aerodynamic efficiency seems difficult to further improve.

Generally it was found that, upscaling using existing materials and design concepts, will result in massive wind turbines that are economically inferior to the existing state of the art. Nowadays, the usage of these methods fail to give an overall impression in conceptual design phase, while technical feasibility and economical characteristics may not be accurate enough to make a realistic judgment about the design (due to the inherent assumptions and simplifications). However, a well

done upscaling approach can give a good initial guess and helps the optimizer to search in a smaller design space, which consequently reduces the overall computational time. Obviously, the main drawback of using an upscaling technique, is the unclear effect that it has on the overall behavior of the turbine. In fact, it must be checked if the trade-off between the higher power production and the mass (and loads) increment is favourable or not. Here an integrated aeroservoelastic simulator comes into play as an useful tool in order to address this issue.

Many integrated simulation tools were developed during the years in order to perform wind turbines design. Examples are *Bladed* from DNV GL [19], or *FOCUS6* from Management Knowledge Centre WMC in cooperation with the Energy Research Centre of the Netherlands (ECN) [32]. As said before, however, this approach is in some way overtaken, and the main trend nowadays is to develop tools that give the possibility to perform a numerical optimization of the wind turbine, following the evolution of desired design requirements. Worthy of note through the actual available panorama are:

- *Framework for Unified Systems Engineering and Design of Wind Plants (FUSED-Wind)* [35] is a free open-source framework for multi-disciplinary optimisation and analysis (MDAO) of wind energy systems, developed jointly by the Wind Energy Department at the Technical University of Denmark (DTU Wind Energy) and the National Renewable Laboratory (NREL). It is build as an extension of the NASA developed OpenMDAO [34].
- *C_p-Max*, developed at Politecnico di Milano, considers a detailed model of the entire turbine and implement complete aero-servo-elastic routines for the design and optimization with the aim of minimizing the cost of energy. A thorough description can be found in Bottasso et al. (2012) [10] or Bortolotti et al. (2016) [7].

Several studies in the ambit of large machines (10-20 MW) were carried on in order to test the effects and potentialities of this type of methods in providing cost-effective design solutions. Thus, many of these studies focus on the modern idea of minimizing the cost of energy. Examples can be the works of Ashuri et al. (2014-2016) [3, 4] which presented a method for the simultaneous optimization of chord, twist, blade length and structural thicknesses, exploring the benefits, challenges and limits in following a general multidisciplinary approach. Again, Bortolotti et al. (2016) [7] present the results of 2 and 10 MW wind turbines design, performed with the holistic approach implemented in the code *C_p-Max*, which exploits the advantages to combine wind turbine macro parameters variations with aero-servo-structural design submodules. Under this point of view,

other significant works that illustrate advantages of multilevel design optimization tools are performed by Zahle et al. (2015) [42], Ning et al. (2013) [37], and Bottasso et al. (2014) [12].

Other works, focus on loads and mass reduction by means of passive and active control systems to achieved lighter wind turbines from the ones derived by up-scaling techniques. For examples, studies regarding bend-twist coupling effects (BTC) on turbine behaviour have been investigated extensively. Lobitz and Veers (1998 and 2003) [30, 31], Cox and Echtermeyer (2013) [17], Vesel and Mc Namara (2014) [41], Stäblein and Hansen (2016) [40], focus attention on the effects of fiber rotation in composite blade components, analysing advantages and limits of this technique. Among others, Croce et al. (2016) [18] cover another type of constructing feature that allows the introduction of bending-torsion coupling effects as demonstrated by Buckney et al. (2014) [13]. In this method, the coupling in the dynamic response of the blade is obtained through the introduction of a geometrical offset between the suction-side and the pressure-side spar cap positions. For what concerns the domain of the active control systems, an individual pitch control (IPC) strategy based on the idea proposed by Bossanyi (2002) [8] is often used, while more sophisticated solutions like flaps and movable tips are currently being investigated. Ultimately, some benefits can be achieved by adopting one or more of these technologies: remarkable examples are fatigue and extreme loads reduction. On the other side, some disadvantages can arise and thus limit the operating exploitation of such devices (e.g. higher manufacturing, installation and maintenance costs).

CHAPTER 2

Optimization problem

This chapter provides an overview of the architecture of $(C_p\text{-Max})$ *A Code for Performance Maximization* [10] developed at Politecnico di Milano.

The program is a numerical tool for the multi-disciplinary optimization of wind turbines and consists in a library of MATLAB subroutines.

The program, however, leans to another software still developed at Politecnico di Milano in order to perform many of the relevant simulations needed in the process: the *Code for Performance, Loads, Aeroelasticity by Multi-Body Dynamic Analysis* $(C_p\text{-Lambda})$ [9]. This aero-servo-elastic simulation tool is able to represent with high-fidelity the static and dynamic behaviour of the machine under all relevant conditions experienced throughout its lifetime. The turbine structural multi-body model is described by means of a series of elements, including non-linear flexible composite-ready beams, rigid bodies, joints, actuators and sensors. A set of aerodynamic models, based on the classical blade-element momentum (BEM) approach formulated accordingly to the annular stream-tube theory, are coupled with the elastic model. They allow to properly consider the aerodynamic characteristics of the blades and to handle several phenomena such as wake swirl, tip and hub losses, unsteady corrections and dynamic stall.

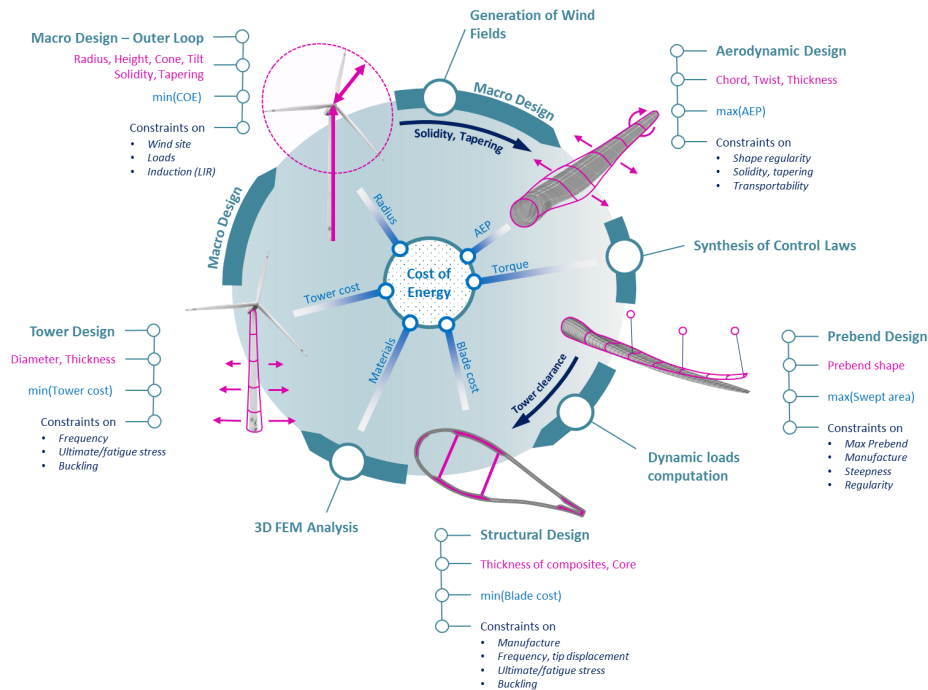


Figure 2.1.1: Overall architecture of the multi-level combined design procedure.

2.1 Overall optimizer architecture

The process flow is organized as depicted in Figure 2.1.1. The main design loop is the Macro Design (or Outer Loop), which allows to optimize high-level characteristics of the wind turbine by targeting at the minimization of the cost of energy. At this level, some of the many parameters of the system are treated as global variables, and in particular rotor radius, hub height, cone and tilt angles, planar and tapering solidities and pitch offset. Each parameter can be arbitrarily included in the set of the Macro design variables or kept fixed, according to the scope and computational resources of the designer. To initialize the Macro Design, a wind turbine macro-configuration must be supplied as initial guess for the optimizer. Then, for each perturbation of the Macro design variables, a full optimization cycle is performed, and a series of Local design submodules are successively encountered. Each submodule is able to perform the detailed design of specific properties of the wind turbine, by targeting at (local) dedicated merit functions. According to the topological scheme of Figure 2.1.1, the main submodules are:

- Aerodynamic optimization tool for the maximization of the annual energy production (AEP).

- Control design tool.
- Blade prebend optimization tool, whose task is the maximization of the rotor swept area in operating conditions
- Structural optimization tool for the blade (and optionally for the tower), whose merit figure is the blade (or tower) cost.

At the end of a global iteration, the annual energy production is re-evaluated for the achieved optimal solution and then the CoE, which represents the Macro objective function of the process, is calculated. The loop continues with a change of the active Macro variables.

Each of the submodules can be run within the global loop or employed as a standalone module to perform the design of specific components of the wind turbine. This modular architecture results advantageous against a traditional monolithic approach for what concerns the overall computational effort during a design process.

It must be noticed how some of the Macro variables play also the role of constraint in the Local optimization steps. For example, the planar solidity of the blade imposed by the external loop is a constraint for the aerodynamic submodule, which then must design the chord distribution in order to achieve that specific solidity.

In any case, both the external problem and the individual optimization submodules are solved by a *Sequential Quadratic Programming (SQP)* algorithm. It is a gradient-based method, which typically assures good convergence properties, and is able to solve the problem:

$$\begin{aligned}
 & \text{find } \mathbf{x} : \min\{f(\mathbf{x})\} \\
 & \text{s.t. : } \quad bl_i \leq x_i \leq bu_i \quad i = 1, \dots, n \\
 & \quad \quad g_j(\mathbf{x}) \leq 0 \quad j = 1, \dots, n_i \\
 & \quad \quad h_j(\mathbf{x}) = 0 \quad j = 1, \dots, n_e
 \end{aligned} \tag{2.1.1}$$

or in other words, finding the set of the design variables $\mathbf{x} = \{x_1, x_2, \dots, x_n\}$ which minimize the objective function f , under some imposed constraints. In order to represent the blade with a sufficient level of detail, a proper choice of the design variables must be made for every sub-problem during the design process. In particular, the total number of design variables must be handled carefully, looking for a compromise between simplicity and completeness or, in other words, between computing time and refinement of the results. In any case some variables

can be considered as frozen if their variation is not desired. This class of optimization methods also ensures a good handling of the constraints which are imposed in order to avoid that non-physical configurations occasionally occur. As shown in Equation 2.1.1 they can be defined in three ways, which correspond respectively to upper and lower boundary values for each design variable, a set of inequality constraints and a set of equality constraints. The first are used for the definition of the extension of the design space, while the others can be linear or non-linear, explicit or implicit functions, and establish if a solution of the problem can be feasible or not depending on their fulfilment. This is the major advantage of this type of methods, since finding a feasible point inside non-linear constrained problems can be a hard challenge to accomplish. A disadvantage can be the high computational time needed for the computation the gradients by means of forward (or centred) finite differences.

In the following, intermediate steps are analysed in-depth, focusing in particular on the choices taken for the design variables in this work, on the constraints and the merit function considered.

2.1.1 Aerodynamic tool

The goal of the aerodynamic optimization submodule is to achieve the highest AEP possible. The latter is defined as:

$$AEP \approx 8760 \sum_{i=cut-in}^{cut-out} P(V_i) f(V_i) \quad (2.1.2)$$

where $P(V)$ is the wind turbine power curve, 8760 is a constant representing the number of hours in a year, and i shows the wind speed range from the cut-in to cut-out, and finally $f(V)$ is the Weibull probability distribution function, used to adapt the power curve to a particular wind site, and defined as:

$$f(V) = \left(\frac{k}{c}\right) \left(\frac{V}{c}\right)^{k-1} \exp \left[- \left(\frac{V}{c}\right)^k \right] \quad (2.1.3)$$

where k is the Weibull shape factor, and c is the Weibull speed scale factor, and are chosen to best match the relevant statistics of a specific wind site. Typical wind energy applications require a given value of k equal to 2, whereas the actual value of the scale factor must be taken according to the wind turbine class following the international standards. It must be noticed that, at this stage, the power curve used for calculate the annual energy production is given as direct analytic evaluation of

$$P(V) = \frac{1}{2} \rho A V^3 C_p \quad (2.1.4)$$

$$C_p = C_p(\lambda, \beta), \quad \text{with} \quad \lambda = \frac{\Omega R}{V}$$

where the power coefficient C_p is computed from Cp-Lambda curves performed at different values of tip speed ratio λ and pitch angles β . Variables governing this problem are contained in the aerodynamic array \mathbf{x}_a , and consist in nodal values for the blade chord, twist and nondimensional thickness. Relative spanwise distributions are obtained by spline interpolation between these values. In particular the nondimensional thickness distribution is obtained by the interpolation of the thicknesses of the given airfoils along the blade, so that changes in their spanwise position are used to modify this variable.

Aerodynamic data along the blade are computed by interpolation from the 2D air tables of given airfoils. Such data are used for the definition of blade lifting lines, which are attached to the elastic multi-body model and follows its deformations during the performed simulations.

The fulfilment of non-linear constraints expressed as

$$\mathbf{g}_a(\mathbf{x}_a) \leq 0 \quad (2.1.5)$$

is required during optimization. These constraints typically account for global limitations such as the maximum allowable tip speed, which in this work is considered to remain ≤ 90 m/s, and the maximum chord. Upper and lower bounds on solidity and tapering for chord and thickness distributions, as well as limitations to the twist distribution (mainly to account for manufacturing constraints), can be given at the same spanwise locations where the nodal unknowns are defined.

2.1.2 Control design

In this work, a dedicated pitch/torque controller was used to regulate the wind turbine during dynamic simulations [24]. Basically, it's a PID-based controller which needs a series of gains and parameters in order to perform the required pitch-torque regulation of the wind turbine.

To provide the data required by the controller, the following procedure is performed: after the aerodynamic design is completed, a simplified steady analysis is run in the operating range of TSR and pitch angles, so that the Cp-Lambda curves are directly computed on the resulting 2D mesh. Based on these results, a regulation strategy is derived as follows:

- a constant TSR strategy for the region II, below the rated power.

$$\begin{aligned}
C_p &= C_p^* = \max(C_p(\lambda, \beta)), & \lambda &= \lambda^*, \\
P &= \frac{1}{2}\rho AV^3 C_p^*, & \beta &= \beta^*, \\
T &= \frac{1}{2}\rho ARV^2 \frac{C_p^*}{\lambda^*}, & \Omega &= \frac{V\lambda^*}{R}.
\end{aligned} \tag{2.1.6}$$

- a constant rotor speed strategy for the region $\text{II}_{\frac{1}{2}}$, in substitution of the classical constant TSR strategy, if imposition on the a limit of the maximum tip speed comes into play in order to reduce the acoustic impact on the surrounding environment.

$$\begin{aligned}
C_p &= \max_{\beta}(C_p(\lambda(V), \beta)), & \lambda &= \frac{\Omega_{max}R}{V} = \lambda(V), \\
P &= \frac{1}{2}\rho AV^3 C_p, & \beta &: \max_{\beta}(C_p(\lambda(V), \beta)), \\
T &= \frac{1}{2}\rho ARV^2 \frac{C_p}{\lambda}, & \Omega &= \frac{V_{tip-max}}{R} = \Omega_{max}.
\end{aligned} \tag{2.1.7}$$

- a constant torque strategy for the region III, above the rated power.

$$\begin{aligned}
C_p &= \frac{2P_{rated}}{\rho AV^3}, & \lambda &= \frac{\Omega_{max}R}{V} = \lambda(V), \\
P &= P_{rated}, & \beta &= \beta(C_p, \lambda), \\
T &= T_{rated}, & \Omega &= \frac{P_{rated}}{T_{rated}} = \Omega_{max}.
\end{aligned} \tag{2.1.8}$$

Here the maximum tip speed represents the only constraint, and consequently the region $\text{II}_{\frac{1}{2}}$ can be present or not in the regulation trajectories.

Then, the necessary data from trajectories, that are the rated rotation speed, and the look-up tables for pitch angle and torque, are updated accordingly in the input files of the controller, while others parameters are given and remain fixed. This allows to automatically update the control laws during the optimization process, in order to follow the evolution of a wind turbine and assure optimal performance at each step. Obviously, during turbulent simulations, variations in the controller variables (i.e. rotor speed, torque and power output) are induced by wind fluctuations, and the PID controller acts on the generator and pitch actuators trying to approach as well as possible the desired performances.

Moreover, in order to handle carefully some particular operating conditions such as shutdowns, startups, emergency braking procedures and faults, another dedicated controller [38] comes into play in substitution to the described one.

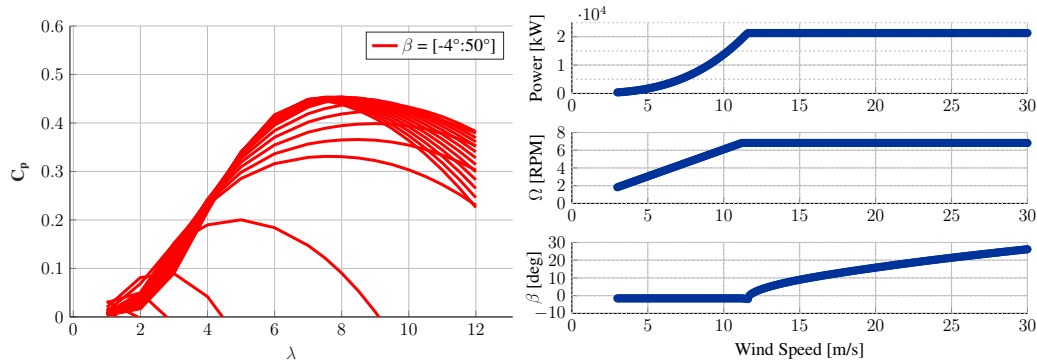


Figure 2.1.2: Example of C_p -Lambda and trajectory regulation curves.

2.1.3 Prebend design

This tool allows the prebend shape to be optimized in order to maximize the rotor swept area considering the blade deformations under rated loads. A detailed formulation of the optimization setup, as well as the application on different rotors is given by Sartori et al. (2016) [39]. The theoretical advantages that could be obtained from a dedicated design of the prebend distribution are a higher AEP, which is caused by the greater rotor area, and a mass reduction due to the higher blade/tower clearance. In modern glassfiber blades, whose design is usually constrained by the maximum deflections, this allows to have a less rigid and thus lighter blade, with positive impacts on the CoE. In a full-field optimization tool like C_p -Max, however, the design variables related to prebend, cone and tilt all concur to the definition of the actual blade/tower clearance. This can result in a badly-conditioned optimization problem and numeric instabilities as well as unrealistic combinations may occur. To circumvent these issues, one can conduct a thorough optimization of the three variables in order to find the best tradeoff without compromising the stability and the general behaviour of the wind turbine. Otherwise, it is possible to conduct parametric studies in which the maximum prebend at tip is constrained and the underlying prebend shape is optimized to meet that boundary. In this work, the global features of the wind turbine are known and fixed, and those include the tilt and cone angles. Thus, the parametric design studies were conducted by following the second approach.

To identify the best distribution, the module describes the desired prebend shape by means of Bézier curves controlled by a defined number of control points. Maximum and minimum values, as like as the local derivatives, can be constrained. The principal reasons to bound these values are the possibility to account for manu-

facture and transportability limits, and the higher general costs of a curved blade, which is not properly considered by the state-of-art cost models considered in this work.

2.1.4 Structural design

This module of the program aims at the minimization of the rotor (and possibly also the tower) cost. The blade structure is described by the definition of the structural elements in terms of planar extension and thickness for all the principal blade structural components (skin, spar caps, shear webs, root, leading and trailing edge reinforcements, core), which are suitably discretized along the blade span. In particular, the positions of the elements are kept fixed, while the thicknesses are contained in the array of the structural design variables \mathbf{x}_s . Initially, the structural rotor properties are evaluated with the finite element cross sectional analysis code ANBA (*ANisotropic Beam Analysis*), implementing the theory of Giavotto et al. (1983) [21]. The result is the six-by-six stiffness matrix, the mass and inertial characteristics, and the location of center of gravity, elastic and shear centers of all the sections at a given spanwise location. Following this approach it is possible to properly account for the anisotropic characteristics of the composite materials, which is fundamental for a correct description of modern thin-layered, high-flexibility wind turbines rotor. With such informations the geometrically exact beam model is updated, and used by the multi-body aero-servo-elastic solver (Cp-Lambda) for running the required aeroelastic simulations. Then, the ultimate and fatigue loads are extracted from the time histories of the simulations by means of various sensors placed in strategic positions in the overall model. Then, considering the given loads, the thicknesses of the blade structural components are optimized under a series of user-defined constraints. Table 2.1 summarizes the set of constraints considered in this part of the optimization process, which takes into account partial safety factors as recommended by the IEC61400 [26] standard. The sizing of the structural elements must address the important topics to satisfy all of these constraints in order to achieve a physically-meaningful solution. The first three constraints act globally, while the others must be satisfied in all the section along the blade where the design variables are defined.

The maximum tip deflection represents the allowable out-of-plane displacement of the blade tip in order to avoid that the blade can crash against the tower and cause irremediable damages. The second regards the 1st flapwise frequency of the blade, that must be higher than the three-per-revolution natural frequency, otherwise their overlapping would lead to a dangerous resonance effects with severe

Table 2.1: Design constraints considered for the blade.

Constraint	Value
Tip deflection	\leq tower-blade clearance
1 st blade flapwise frequency	$\geq 3P$
1 st edgewise frequency	$\geq 1^{\text{st}}$ flapwise frequency
Maximum ultimate stress	\leq Allowable stress
Fatigue damage index	≤ 1
Buckling eigenvalues	≥ 1

consequences in the total fatigue loads. Both these constraints are strongly linked to the out of plane stiffness of the blade and widely influence the sizing of the structural elements, especially for large rotor. In particular, due to the huge turbine high-rise, the effects of the vertical shear of the mean wind profile has a relevant influence on the blade loads. For this reason, in this design, the maximum tip deflection constraint has been considered only for azimuth positions of each blade close to the tower (with an angle of $\pm 30^\circ$ from its axis), allowing the blade to have higher deflections in the upper part of the rotor disc, and the result is a more flexible and lighter blade than that obtained by classical upscaling.

Once again, the bound on the ratio between the 1st edge and 1st flap blade frequencies is imposed to avoid possible couplings effects, which might possibly lead to resonance phenomena.

The last constraints concern structural safety tests that must be satisfied in order to guarantee the integrity of the blade. Hence, the elements thicknesses of the optimized blade must be sized to withstand ultimate and fatigue loads deriving from all the possible working conditions.

If tower optimization is included in the process, similar constraints must also be satisfied at each tower section. Furthermore, a constraint on the gap between the three-per-revolution natural frequency and the first system frequency (which is drive right from the tower properties) have to be guaranteed, again to avoid resonance effects.

Eventually, a detailed finite element method (FEM) model of the blade can be built, and used to capture the three-dimensional stress and strain state with a higher level of precision. It allows to ensure that all desired structural constraints are verified by means of static, modal and fatigue analyses, that use loads computed at the aeroservoelastic level. Then, the structural thicknesses and the corresponding boundaries are updated for the next aero-elastic iteration.

2.1.5 Objective function

The common practice in design optimizations of wind turbine during the last years is to use the Cost of Energy (CoE) as objective function. The main advantage in using this metric is the fact that all the main cost-influencing design variables of the turbine can be easily taken into account in its definition. This is a useful characteristic especially in a multi-disciplinary approach, in which thanks to the overall nature of the cost of energy, each aspect considered in the design can directly influence the merit figure of the optimization process. In this work a dedicated cost model developed within the INNWIND.EU consortium [25] was employed. Such model was formulated for multi-MW next-generation offshore wind turbines and it's a refinement of the original scaling model developed by NREL [20] for this category of turbines. All the main costs for the elements of the turbine are evaluated starting from the description of the structure, of the materials used, and of some wind turbine macro-parameters such as rated power and rotor diameter. The common definition of the CoE (or Levelized Cost of Energy, LCoE) is:

$$\text{CoE} = \frac{\text{FCR} * \text{ICC}}{\text{AEP}_{\text{net}}} + \text{AOE} \quad (2.1.9)$$

where principal key players are the Fixed Charge Rate, Initial Capital Cost, Net Annual Energy Production and the Annual Operating Expenses.

A highly detailed blade cost model (BCM) developed at Sandia National Laboratories by Johans and Griffith (2013) [22] is also implemented in the code, and takes into consideration the real costs of materials, labour and equipment used during the manufacturing process of the blades.

It must be noticed that, at this preliminary stage of the design process, basing the work on the minimization of the CoE may be an unsuitable choice for many reasons. First of all, there aren't many other similar studies regarding 20 MW WT which can be used as a benchmark: then, a thorough minimization of the loads and component masses must be performed ahead of targeting a reduction of the cost of energy. Second, a complete redesign of other components of the turbine must to be performed in order to completely appreciate the advantages of the design of the new rotor, in terms of CoE variations. Since this works focuses instead on the rotor design, it is our opinion that the expected advantages coming from redesign of i.e. tower and foundations could not be properly accounted for. Future developments of this activity will focus on integrated cost-reduction strategies, as well as detailed redesign of all the turbine components.

According to this logic, the focus during the various design steps performed in this work was to minimize the rotor mass and the key loads experienced by the turbine

components. Since many cost models tightly relate the blade cost to its mass, targeting the mass has also a direct impact on the overall Turbine Capital Cost, and thus on the CoE. In this way, possible future advantages deriving from complete re-design of the turbine can be, even if indirectly, taken into consideration. Furthermore, changes in the blade aerodynamic and structural design parameters at frozen global wind turbine configuration (e.g. at fixed rotor diameter), as in the proceeding of this work, significantly affect AEP, mass, loads, etc., but appeared to affect the CoE merit figure in a limited way.

Anyway, a CoE evaluation is consistently used to assess the economical feasibility of the turbine and identify the trade-off between the rotor performance and the structural integrity.

2.2 Certification guidelines

Since this work is focused on a preliminary design of the turbine, a reduced set of design loads cases (DLCs) is considered during the optimization design process in order to achieve an acceptable computational time. However, the choice of the DLCs is done by taking into consideration all the possible operating conditions that a wind turbine encounters throughout its lifetime, so that, a meaningful solution can be reached. As a further simplification, turbulent DLC were performed with only one seed although, in real-world applications, several seeds are required for a comprehensive analysis.

The design load cases are summarized in Table 2.2, according to their definitions as specified by the International Electrotechnical Commission, 2006 [26]. All the cases contribute to the definition of the ultimate loads, while only the normal power production condition is taken as a driver for the fatigue equivalent loads, as they are representative of the normal working condition of the machine.

Turbulent wind time histories are generated with the open-source code *TurbSim* [29], while deterministic gusts are generated according to international standards.

Table 2.2: Design load cases

DLC	Wind type	N. of seeds	Wind speed [m/s]	Yaw misalignment [deg]	Fault	SF
1.1	NTM	1	$V_{in} : V_{out}$	-	-	1.35
1.3	ETM	1	$V_{in} : V_{out}$	-	-	1.35
2.1	NTM	1	$V_{in} : V_{out}$	-	Grid loss	1.35
2.3	EOG	-	$V_{r-2}, V_r, V_{r+2}, V_{out}$	-	Grid loss	1.1
6.1	EWM	1	V_{ref}	-8,0,+8	-	1.35
6.2	EWM	1	V_{ref}	-180:30:180	Grid loss	1.1

CHAPTER 3

Models

In this Chapter, the starting model of the 20 MW wind turbine will be presented, in order to give an overall description of its relevant characteristics. Such model, hereafter referred as Reference 20 MW, was derived from the 10 MW RWT [5] by applying classical upscaling techniques in a first modelling step. Afterwards, corrections were performed to adjust up-scaled data considering learning curve expectations. Attention was paid in particular to what concerns components masses and the proper selection of the first systems' frequency. A more complete description of the upscaling work can be found in the dedicated report [16] and through reference therein.

After that, a preliminary structural redesign of the wind turbine, referred as Baseline 20 MW, will be shown in detail. Fundamental features in terms of blade properties, performances and occurred loads will be analysed and compared with the Reference 20 MW model. At this step, since the focus is on the structural tuning of the rotor design, several high-level characteristics of the turbine are left unchanged during the optimization process: these include rotor radius, hub height, the aerodynamic definition of the rotor as well as the aero-structural description of hub, nacelle and tower.

3.1 Reference 20 MW model

The essential features of the 20 MW wind turbine are listed in Table 3.1. The machine is based on the IEC-61400 class IC, whereas the 10 MW RWT which is a class IA. This difference implies a lower magnitude of the expected wind turbulence in operating conditions. This aspect was duly taken into account during the correction step made on the upscaled data, since it influences the design of some turbine components. In particular, a first direct implication is a relative reduction of the expected fatigue loads, which are the design drivers of some important turbine subcomponents like for example the main shear webs and the tower segments. As a consequence, the mass scaling factors for the hub, drive train and nacelle were assumed lower than cubic. Other parameters have remained unchanged during the upscaling process, that is, orientation, control type, cut in/out speeds, rated wind speed, number of blades, maximum tip speed, cone and tilt angles.

Table 3.1: Overall characteristics of the wind turbine.

	Class	IEC IC
Rotor orientation		Clockwise, upwind
Control		Variable speed, collective pitch
Cut in speed		4 m/s
Cut out speed		25 m/s
Rated wind speed		11.4 MW
Rated power		20.0 MW
Number of blades		3
Maximum Tip Speed		90.0 m/s
Cone angle		2.5°
Tilt angle		5°
Rotor radius		126.1 m
Hub Radius		3.95 m
Hub height		167.9 m
Tower height		163.17 m
Blade mass		117849 kg
Hub mass		278470 kg
Nacelle mass		1098270 kg
Tower mass		1779190 kg
Generator Inertia About Shaft		8488.1 kg/m ²
Electrical Generator Efficiency		94%

3.1.1 Blade description

In the following, characteristics of geometry, mass, stiffness and inertia are given for the blade. No significant deviations from the classical upscaling theory are considered here, under the assumptions that usual scaling laws can provide a sufficiently accurate starting point for a subsequent integrated design approach.

A set of airfoils belonging to the FFA-W3 family is defined along the blades at specific pivotal stations. The airfoil shapes are identical to those employed for the definition of the 10 MW RWT model is used. These airfoils were studied specifically for wind turbines and their geometrical and aerodynamic characteristics are publicly available from the original paper (Björk 1990 [6]). A peculiarity of these airfoils is the relatively high thickness, which therefore provides high sectional inertia and chordwise stiffness. This ultimately allows the design of a relatively lightweight blade. However, since existing FFA airfoils are defined in a range of thickness between 21.1% and 36.0%, during the design of the 10 MW RWT additional airfoils were created. In particular, due to the high request of flapwise stiffness related to the high blade length, a first airfoil with 48% thickness was created from a simple multiplication of the normal-to-chord coordinates of the 36% airfoil. Afterwards, a transitional airfoil with thickness of 60% was created through an interpolation between the 48% airfoil and the cylindrical root section. CFD analysis were performed on the airfoils in the range of required Reynolds numbers ($6-12 * 10^6$).

In this work the same characteristics are used, under the assumption that airfoil polars do not scale with respect to the radius, and effects of higher Reynolds numbers due to the larger chords can be neglected. However, the 60% airfoil was eventually not considered in our design process, since available polar data show unexpected bumps in the vicinity of the null angle of attack. As demonstrated during the INNWIND.EU activities, this feature can trigger numerical instabilities in several simulations. Aerodynamic properties of the blade between the root and the first pivotal airfoil (48%) were then obtained by direct interpolation. A list of airfoils and their non-dimensional positions along the blade is reported in Table 3.2.

Relevant geometrical and aerodynamic properties of the airfoils can be found in Chapter 3 of the DTU 10MW RWT datasheet.

The main aero-structural properties of the blade are depicted in Figure 3.1.1 and Figure 3.1.2. Geometrical planform characteristics have been scaled-up proportionally with the radius, while higher-order exponential are assumed for the other properties depending on their definitions. The twist distribution is on the contrary independent from the scale of the rotor, since its definition depends on the actual

Table 3.2: Blade airfoils.

Number	Airfoil	Thickness %	Nondimensional spanwise position %
1	Cylinder	100	0
2	Cylinder	100	1.74
3	FFA-W3-480	48	20.80
4	FFA-W3-360	36	29.24
5	FFA-W3-301	30.1	38.76
6	FFA-W3-241	24.1	71.87
7	FFA-W3-241	24.1	100

aerodynamic inflow at each station. The resulting sectional thickness is calculated from the chord distribution and the non-dimensional thickness along the blade: the latter was, as mentioned, derived by interpolating the thickness of the pivotal airfoils.

3.1.2 Tower description

In typical applications, the tower height is not up-scaled with a SF equal to 1 (which implies a linear scaling with respect to the radius), since this is not the best cost effective strategy. Instead, it is defined in a way which maintains the blade-to-ground clearance within a prescribed level. In the definition of the Reference 20 MW, the tower is then derived by first linearly up-scaling the reference tower and then by cutting its bottom part as much as needed to match the desired hub height.

However, after some considerations, the tower is further elongated of 12 meters in order to reduce the first frequency of the system, and avoid interactions with the three-per-revolution natural frequency at low speeds. This workaround moves resonance effects toward even lower wind speeds, leading to a higher energy capture and a reduction of the fatigue loads. In fact, although a longer tower increases the ultimate and fatigue moments on the support structure, this will be counter-balanced by the suppression of the dynamic loads.

Distributed properties of the tower structure are showed in Figure 3.1.3. The structure is assumed to be made of 10 tubular sections, each with a constant thickness and a linear decreasing external diameter distribution.

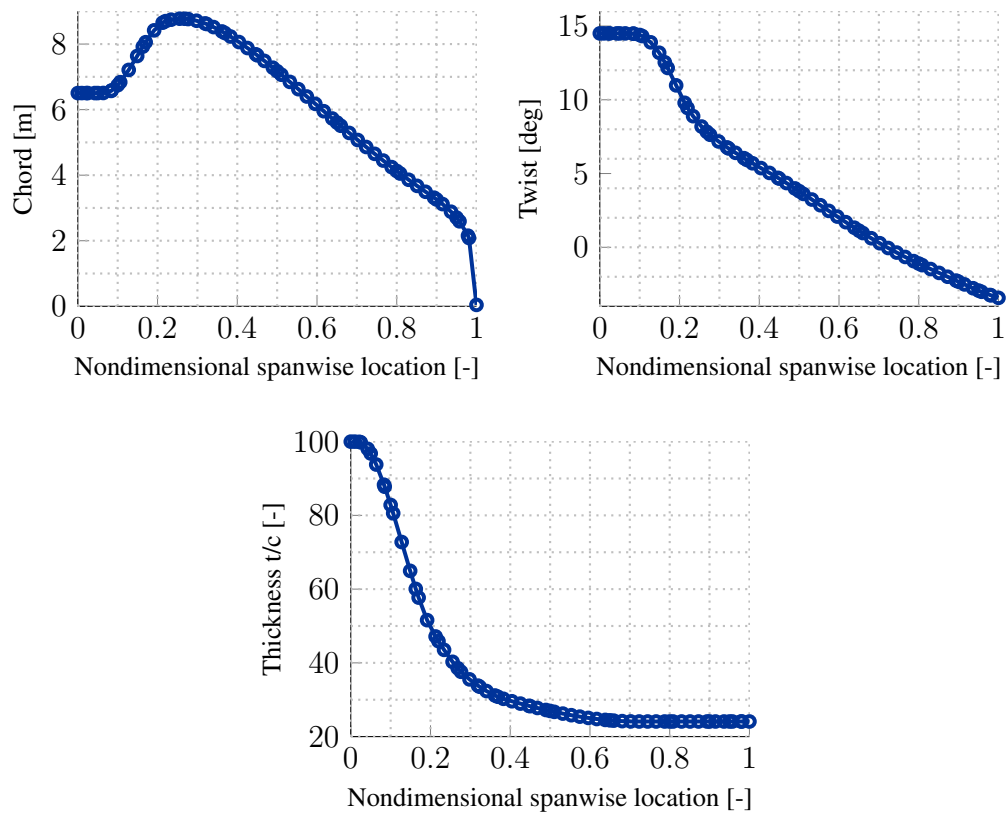


Figure 3.1.1: Reference 20 MW blade geometrical properties.

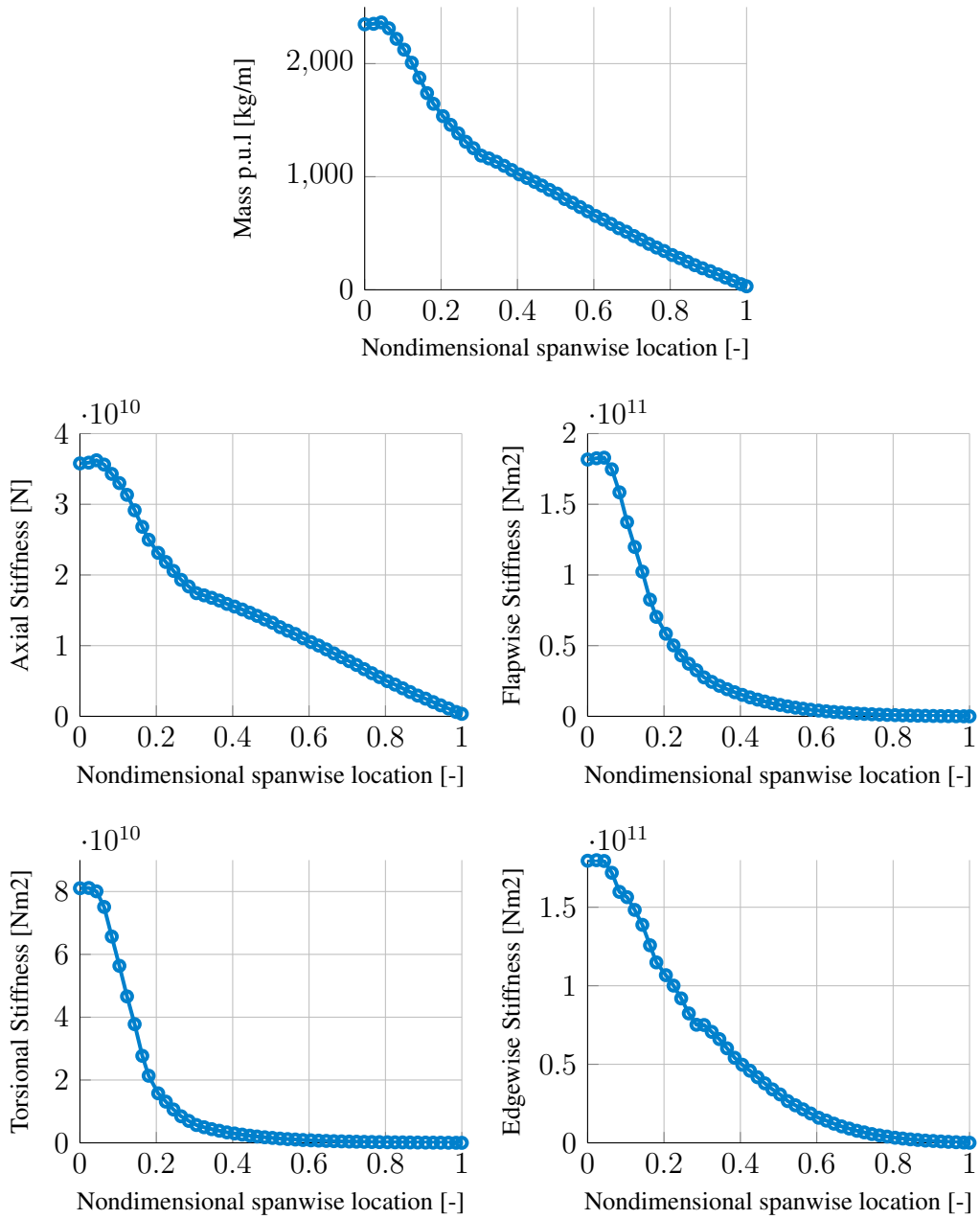


Figure 3.1.2: Reference 20 MW blade mass and stiffness properties.

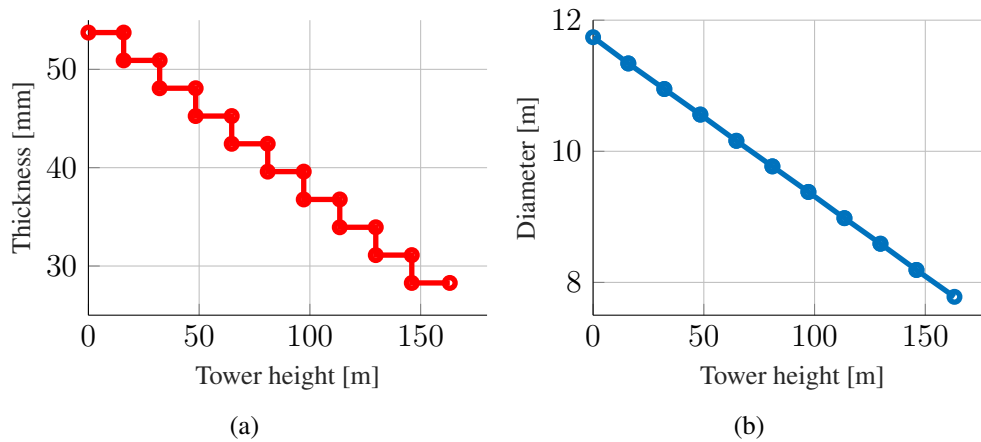


Figure 3.1.3: Tower thickness and diameter distributions.

3.1.3 Control

A similar scaling approach has been used for the determination of the controller parameters, which have been computed starting from the settings applied on the 10 MW RWT. A first round of classical linear scaling laws was applied, followed by a second step in which the data were corrected on the basis of previous experience.

In particular, a great care was taken in the definition of a suitable minimum rotor speed. This value is usually determined by the performance of the generator, and in particular by the maximum braking torque which can be supplied by the system. However, in this study, this theoretical value was increased by a 5%, so that the minimum rotor speed is slightly higher than expected. This trick was used, together with the tower modification, to shift dangerous resonance effects towards the lower part of the operating wind speeds, where the consequences in terms of fatigue are less severe. This embedded protection strategy, however, has consequences on the power production, which is forcibly reduced at low speeds.

On the contrary, the optimal rotational speed targeted by the supervisor is always computed from the illustrated trajectory regulation laws, which are recursively re-evaluated at each design step.

3.2 Baseline 20 MW model

Once that the aero-elastic definition of the Reference 20 MW was completed, a preliminary design of the internal structural layout of the 126m-long blades was performed. The main goal of this phase was then to identify an efficient and physically feasible sizing of the structural components in order to meet the properties of the Reference 20 MW as close as possible. To this aim, the internal structural topology was initially defined and subsequently a mass-minimization optimization procedure was carried out by means of the C_p -Max structural submodule. As a consequence, the optimal configuration automatically satisfies the set of nonlinear constraints required by certification standards and discussed earlier. The first step was the definition of each structural elements in term of its span-wise location and chord-wise extension. As a starting point, a simple stretching of the 10 MW structural redesign performed by PoliMI in the context of the INNWIND.EU project, was considered. The optimal thickness of each structural components was then computed by the optimization algorithm. However, after a preliminary re-sizing, an excessive (for manufacturing process) spar cap thickness was obtained by the optimizer. This required to modify the length and width of the suction-side and pressure-side spar caps, which were basically widened and elongated. It must also be noticed how the spar caps are enlarged in the root area in order to increase the local stiffness and redistribute the loads across the overall section. The final blade planform is represented in Figure 3.2.1. The golden dotted line highlights the location where an additional layer of unidirectional glass fiber known as *root reinforcement* ends. As many blade design based on glassfiber fabrics, the main design driver for the internal structure, and in particular for the spar caps, is the maximum tip deflection.

The structural arrangement of the blade is based on a classic three-cells section with a spar box and two identical shear webs. A third shear web was introduced in order to reduce the free-length of the shell panels and to retard the onset of buckling. As shown in Figure 3.2.2, different sectional elements, or panels, are defined along the blade at each required section: each element is associated to a lamination sequence which accounts for the correct stacking sequence of different materials, mainly composite fabrics and fillers. In particular, there are:

- Four shell panels (composed by a sandwich of triaxial texture coated together with balsa),
- Two spar caps elements (made up of unidirectional glassfiber),
- Two main shear webs (biaxial/balsa sandwich arrangement),

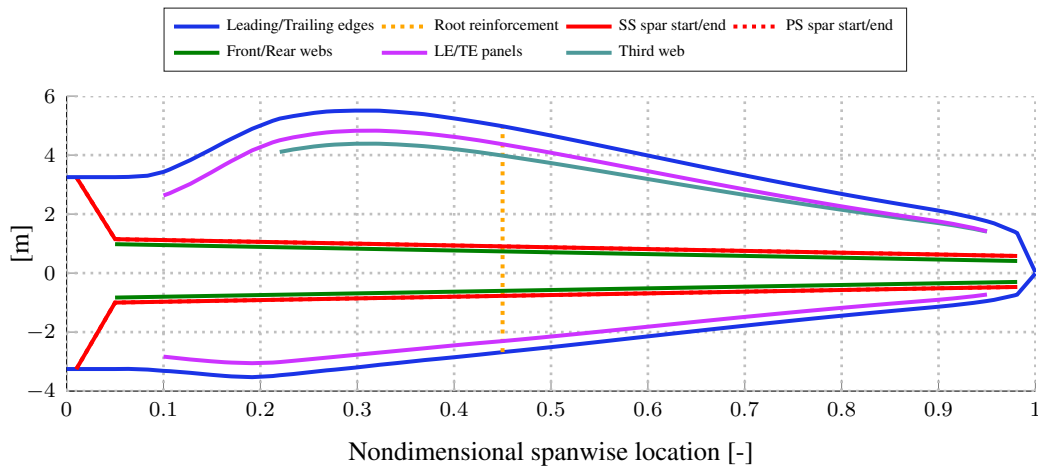


Figure 3.2.1: Baseline 20 MW blade planform.

- Leading edge and trailing edge reinforcements (unidirectional),
- A third shear web (triaxial),
- A root reinforcement in the vicinity of the root (unidirectional).

All the elements contribute to the general blade characteristics, but specific tasks can be identified for each one. Shell panels maintain the aerodynamic shape of the airfoils in order to guarantee their aerodynamic performance, and take care of the torsional loads together with webs. The latter are also responsible of absorbing the shear loads, but they are also meant to alleviate buckling phenomena by reducing the free-length of the spar panels. Spar caps bear most of the flapwise bending, since they are the main contributors to the out-of-plane stiffness of the blade. In this sense, the root reinforcement plays also a contribute by providing a higher global stiffness in the initial root area and promoting a better redistribution of the loads managed by the spar caps. A third web is added near the trailing edge in order to toughen the blade section and helps in manage buckling phenomena. Finally, the leading and trailing edge reinforcements help in afford in-plane stiffness of the rotor and taking care of edgewise loads. The mechanical properties of the various composite materials are defined accordingly to the datasheet of 10 MW RWT reference wind turbine, and reported in Table 3.3.

The optimization variables in the design process are the individual thicknesses of each structural components defined at 18 significant sections along the blade span. These are listed in Table 3.4. At these locations, corresponding upper and lower bounds for each variables are set. Starting from these sections, both thick-

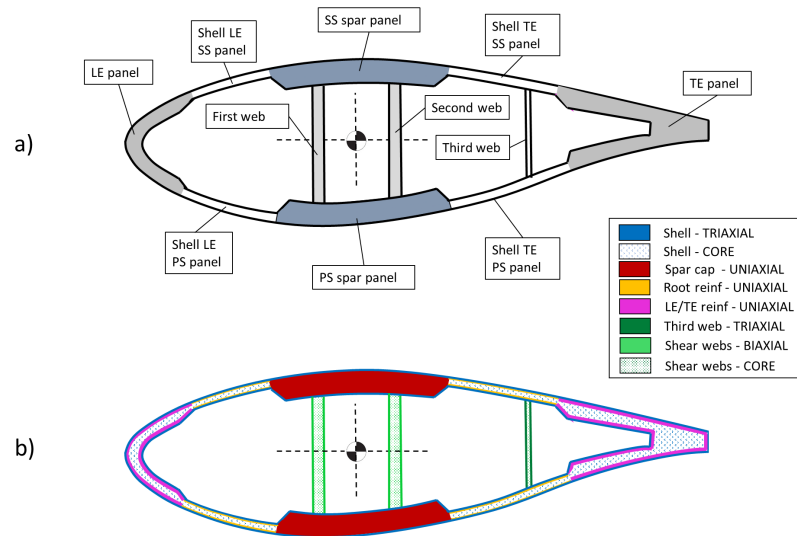


Figure 3.2.2: Internal blade layout: sectional elements (a) and structural components (b). Note: leading edge LE; trailing edge TE; suction side SS; pressure side PS.

Table 3.3: Blade material properties.

Property	Units	Unidirectional	Triaxial	Biaxial
E_{11}	[GPa]	41.63	21.79	13.92
E_{22}	[GPa]	14.93	14.67	13.92
ν_{12}	[-]	0.241	0.478	0.533
G_{12}	[GPa]	5.047	9.413	11.50
ρ	[kg/m ³]	1915	1845	1845
σ_{xmax}	[MPa]	876.1	480.4	223.2
σ_{xmin}	[MPa]	625.8	393	209.2

Table 3.4: Structural design optimization sections of the blade.

Section number	η	Section number	η
1	0	10	0.323
2	0.010	11	0.369
3	0.025	12	0.450
4	0.050	13	0.500
5	0.083	14	0.650
6	0.100	15	0.800
7	0.163	16	0.900
8	0.220	17	0.950
9	0.268	18	0.981

Table 3.5: Mass, AEP and CoE comparison between Baseline and Reference models.

	Mass [kg]	AEP [GWh/yr]	CoE [\$/MWh]
Reference 20 MW	117848	90.80	86.33
Baseline 20 MW	113505 (-3.7%)	91.62 (+0.9%)	84.92(-1.6%)

nesses and bounds are linearly interpolated to get a finer characterization of the blade. The detailed mesh consists of 65 sections in which mass, stiffness and inertia properties are defined. At each station, the local constraints described in section 2.1.4 must be satisfied. In this way is possible to handle an optimization process with a relatively limited number of variables, which implies a lower computational time, without losing the high-fidelity that is required by the multi-body description of the wind turbine model.

The optimized blade, named Baseline 20 MW, results to be lighter and with a higher AEP capture with respect to the Reference one. This is globally reflected by a better CoE, as shown in Table 3.5. However, the performances of the two models are very close and somehow confirm expectations against the upscaling model in particular for what concerns the estimation of the mass.

Turbulent power curve obtained from simulations of the DLC 1.1 is depicted in Figure 3.2.3, together with the corresponding power coefficient. As discussed, the energy capture at low wind speeds is limited due to the lower bound imposed on the rotation speed. To improve the AEP in this range of wind speeds, a pitch angle different from the optimal one could be used, depending on the regulation curves. In this re-design, however, this problem has not been addressed and could be investigated in future works. In Figure 3.1.3 the resulting thickness distributions of the optimized blade elements for the Baseline 20 MW are depicted. At the same

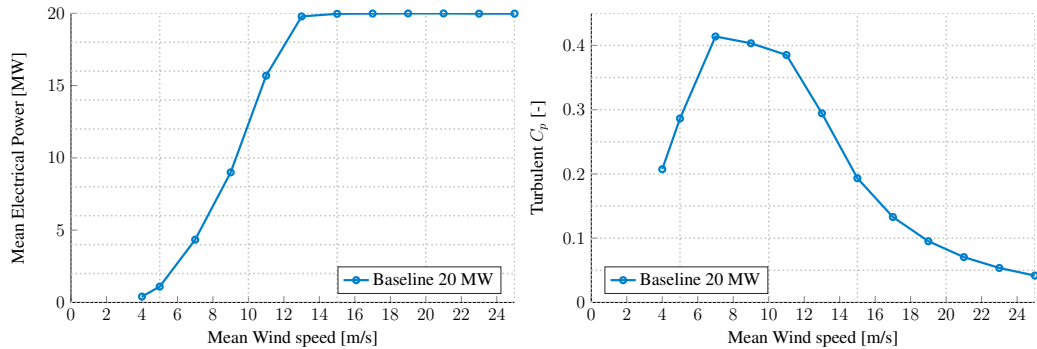


Figure 3.2.3: Turbulent power curve and power coefficient.

time the lamination sequence described previously can be observed in detail. As it can be seen in Figure 3.2.5, the final structure of the Baseline 20 MW reproduces quite well the blade properties of the Reference 20 MW aero-elastic model, at least within the limits of an engineering point of view. In particular, there is a good match between the two rotors in the outboard part of the blade. On the other side, in the vicinity of the root, the optimizer leads to a solution that differs significantly from the reference one. This is mainly due to the root thickness, which has been constrained in $C_p\text{-Max}$ to (preliminarily) account for the root solution (root inserts) which will be detailed in future activities. However, this mismatch is not very important considering that the Reference aero-elastic model is an ideal and theoretical representation of the characteristics of the blade and not a real and feasible solution. However, it is interesting to notice how the upscaling model used is able to provide a valid starting point for the design of the turbine, since the initial guess for the thickness distributions was made to approach as close as possible those stiffness distributions. This observation is valid also for the mass distribution and, consequently, for the total mass of the blade as illustrated in Table 3.1.

These considerations justify the good agreement in design loads when DLC simulations are performed for the two models. In Table 3.6 and Table 3.7 the ultimate load and the equivalent fatigue loads (DEL) detected by the Baseline 20 MW are compared with respect to those developed by the Reference 20 MW. It can be noticed that most key loads agree fairly well within the set of considered DLC. Exceptions are the bending moments at the tower root that is significantly higher in the second case. The root causes for this discrepancy should be analyzed and corrected in a subsequent tower optimization. For the continuation of this work, however, the agreement in the range of $\pm 15\%$ is considered broadly acceptable so that the aero-structural properties of the tower were not modified.

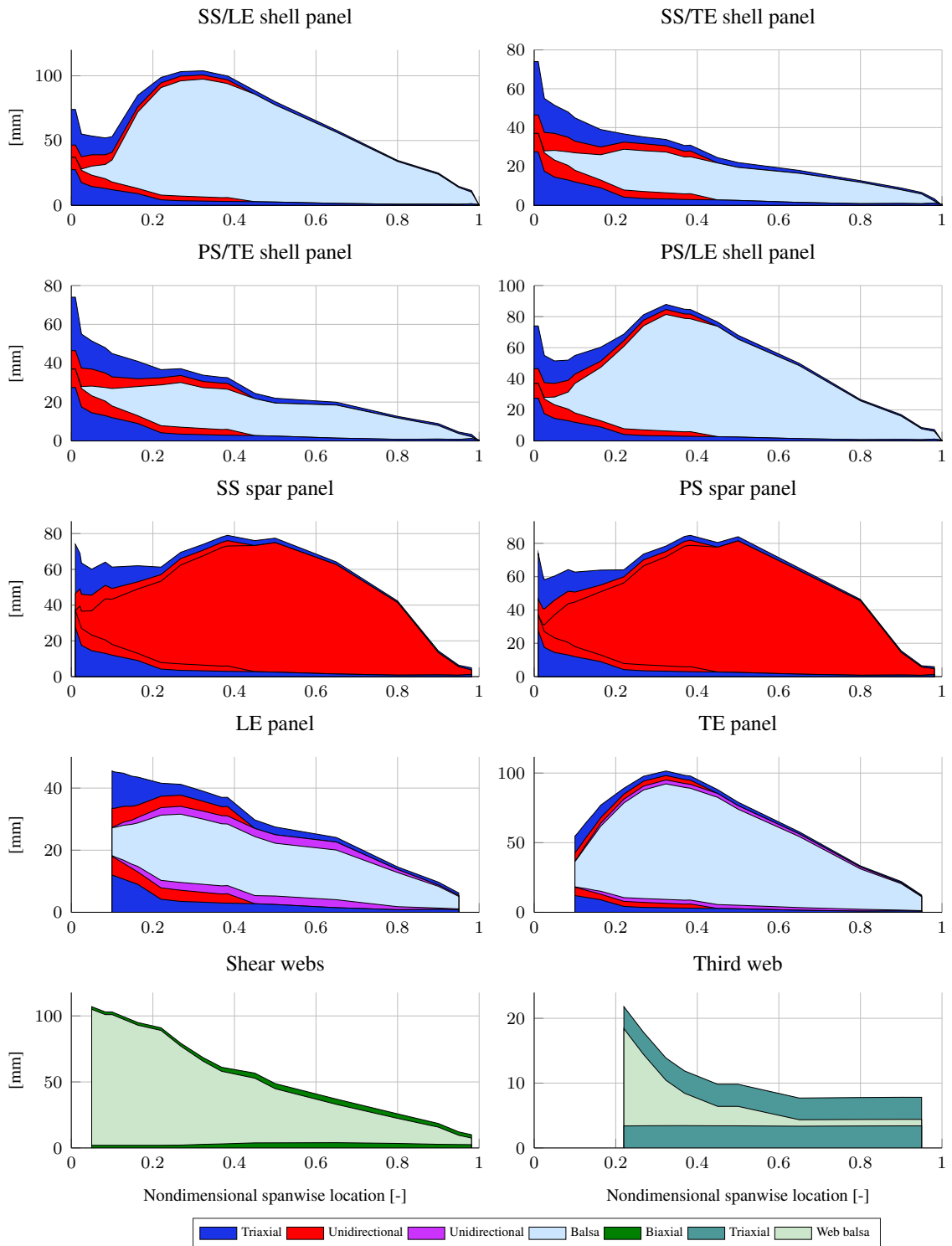


Figure 3.2.4: Thickness distributions and lamination sequence of the blade elements for the Baseline 20 MW.

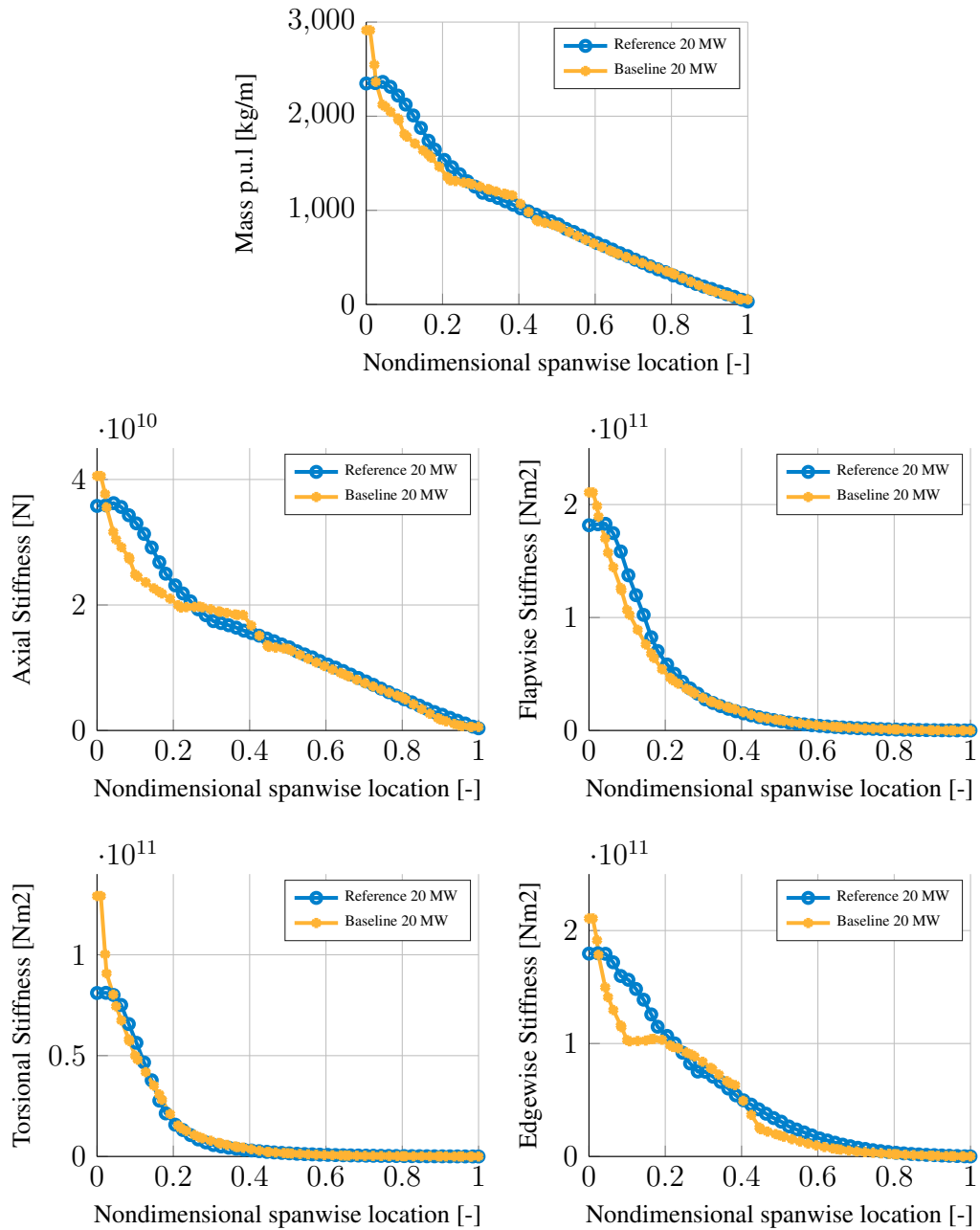


Figure 3.2.5: Baseline 20 MW blade stiffness properties compared with the Reference 20 MW ones.

Table 3.6: Ultimate loads comparison between Reference 20 MW and Baseline 20 MW.

Sensor	Load	Units	Reference 20 MW	Baseline 20 MW	Δ %
Blade root	Edgewise bending	[kNm]	100207 DLC 23- V_r	106519 DLC 23- V_r	+6.3
	Flapwise bending	[kNm]	174756 DLC 13-11m/s	168979 DLC 13-11m/s	-3.3
	Combined Flap/edge	[kNm]	174759 DLC 13-11m/s	172792 DLC 13-11m/s	-1.13
	Torsion	[kNm]	1706 DLC 23- V_r	1521 DLC 62-yaw-60°	-10.8
Hub	Thrust	[kN]	5703 DLC 13-11m/s	5757 DLC 13-15m/s	+0.95
	Nodding moment	[kNm]	106968 DLC 13-25m/s	104573 DLC 13-19m/s	-2.23
	Yawing moment	[kNm]	97069 DLC 62-yaw-30°	86603 DLC 13-25m/s	-10.8
	Combined Nod/yaw	[kNm]	115709 DLC 62-yaw-30°	112913 DLC 13-19m/s	-2.42
Tower base	Fore-aft moment	[kNm]	1316548 DLC 62-yaw 90°	1480055 DLC 23- V_r +2	+12.4
	Side-side moment	[kNm]	1078489 DLC 62-yaw-30°	1244365 DLC 62-yaw-30°	+15.4
	Combined FA/SS	[kNm]	1467017 DLC 62-yaw-30°	1480421 DLC 23- V_r +2	+0.91
	Torsion	[kNm]	99075 DLC 13-25m/s	93180 DLC 13-25m/s	-5.95

Table 3.7: Fatigue DEL loads comparison between Reference 20 MW and Baseline 20 MW.

Sensor	Load	Units	Reference 20 MW	Baseline 20 MW	Δ %
Blade root	Flapwise DEL	[kNm]	73319	84376	+15.1
	Edgewise DEL	[kNm]	99602	97133	-2.48
	Torsion DEL	[kNm]	1550	1378	-11.1
Hub	Thrust DEL	[kN]	1208	1372	+13.6
	Nodding DEL	[kNm]	50207	54753	+9.05
	Yawing DEL	[kNm]	47623	50432	+5.89
Tower base	Fore-aft DEL	[kNm]	255918	288485	+12.7
	Side-side DEL	[kNm]	164693	223310	+35.6

CHAPTER 4

Optimization studies

In this Chapter the results of the optimization studies performed on the Baseline 20 MW will be showed, focusing in particular on the progressive load alleviation and blade mass reduction. The logic path is depicted in Figure 4.0.1, and in each block the investigated solutions were redesigned using dedicated C_p -Max design submodules as described in the optimization procedure, so that the achieved solutions satisfy at each step the identical design constraints. As it can be seen, starting from the Baseline 20 MW rotor an optimal prebend distribution was initially investigated, followed by the introduction of passive and an active control methods, which are based on the concepts of the Fiber-induced Bending-Torsion Coupling (F-BTC) and the Individual Pitch Control (IPC) regulation. Finally a study on planar solidity was carried out in order to possibly improve the aerodynamic performance of the rotor.

During the process, the best configuration obtained in each individual study has been taken as the initial guess for the next one. In this way, the benefits emerging at each steps are integrated in the final configuration. Due to the nature of this study, it has been judged that this modular approach allows a better compromise between insight in the results and computational effort against a more traditional, monolithic approach to the optimization problem, in which all the design variables are managed by the optimizer at once. Future developments of this work

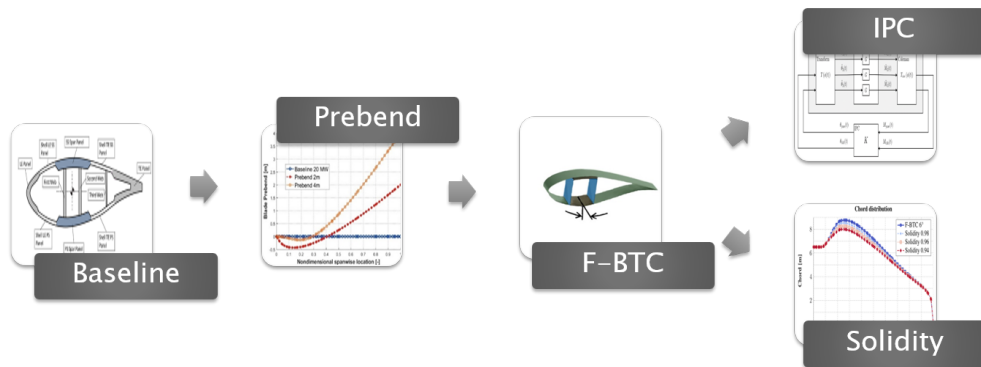


Figure 4.0.1: Optimization analyses process flow.

will focus on a completely automated redesign of the wind turbine in the context of a classical optimization methods. This could confirm, and possibly extend, the findings of this preliminary design activity.

4.1 Prebend

The first parametric study aims at the identification of an optimal configuration for the prebend distribution along the blade. Starting from the Baseline 20 MW, a complete structural optimization loop for varying values of tip prebend was performed. To consider current manufacturing limits, only the tip prebend values of 2 and 4 meters were considered, since a higher level of freedom could lead to an unrealistic amount of curvature in certain parts of the blade. The resulting distributions are showed in Figure 4.1.1, together with their direct impact on the computation of blade-tower clearance.

Only the structural optimization was performed at this step, under the hypothesis that a variation in the prebend distribution does not affect significantly the aerodynamic performance of the blade. Although this is reasonable for a static estimation of the AEP, a different prebend can indeed modify the dynamic behaviour of the rotor in turbulent conditions, leading to some differences in the corresponding AEP. Than, in order to avoid energy losses, the AEP obtained from turbulent DLC 1.1 is continuously monitored in this step.

Results confirm the theoretical predictions, as one can see in Table 4.1. The mass of the blade is the most affected parameter and its decrease follows quite well the prebend variation. On the contrary, the AEP increases in both cases, however the increase is limited in the second case, probably due to the influence on the turbulent power production of the higher deformations allowed by the lower

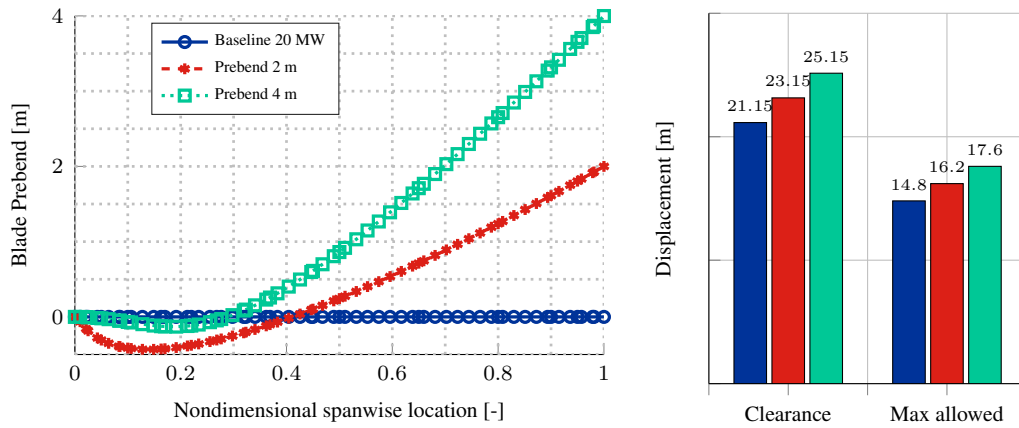


Figure 4.1.1: Prebend distributions and consequent variation of the blade-tower clearance.

Table 4.1: Mass, AEP and CoE comparison between Prebend solutions and Baseline 20 MW.

	Mass [kg]	AEP [GWh/yr]	CoE [\$/MWh]
Baseline	113505	91.62	82.64
Prebend 2 m	110135	91.89	82.43
Prebend 4 m	107446	91.80	82.44

flap stiffness. The combination of these two factors leads to a similar CoE improvement with respect to the Baseline 20 MW model. For what concerns the loads, during this work some fundamental load metrics as important design driver are considered. These include the multi-directional combined bending and the corresponding fatigue DELs at blade root, hub and tower. Figure 4.1.3 shows percent variations for the two cases under investigation with respect to the Baseline 20 MW. Results show that ultimate loads are globally higher, even though the increase is lower for the 4m case. However, all loads are in a range of $\pm 5\%$ from the Baseline 20 MW, with the only exception of the combined fore-aft/side-side bending at tower top, which is increased. Analysis of the fatigue DELs, on the contrary, show an inverted trend, as most of the key loads are significantly decreased. The fore-aft DEL at the tower base increases, but the percent variation is below the threshold of 10% from the Baseline 20 MW.

At the end of this step, the model with a 4 m prebend was considered the one that exhibits the best overall performances and was then assumed as the initial guess for the next study.

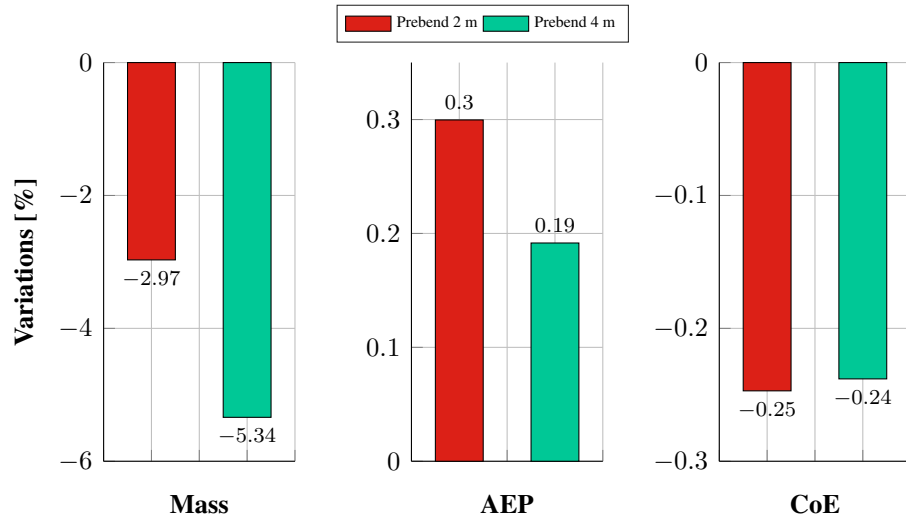


Figure 4.1.2: Performance percentage variation with respect to the Baseline 20 MW model.

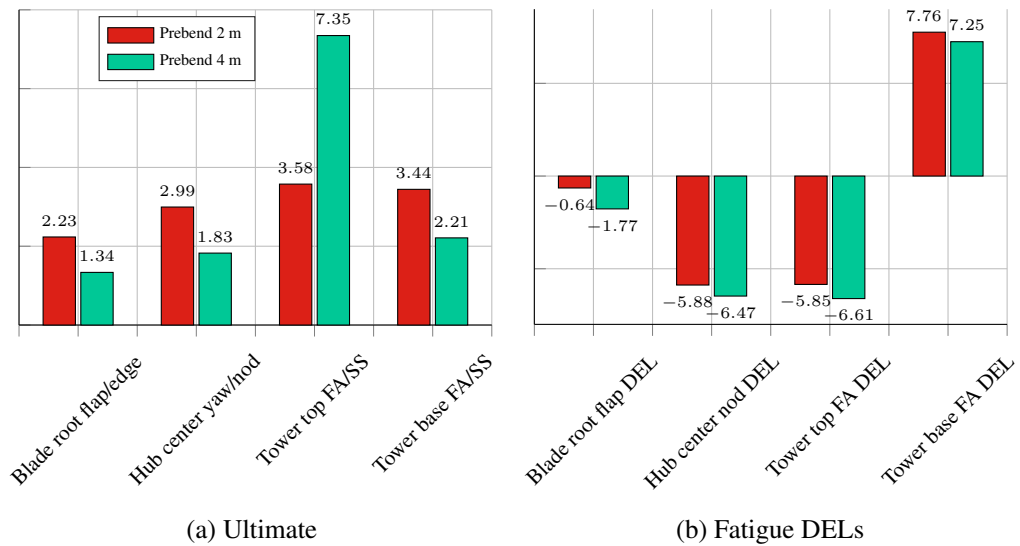


Figure 4.1.3: Key loads percentage variation with respect to the Baseline 20 MW model.

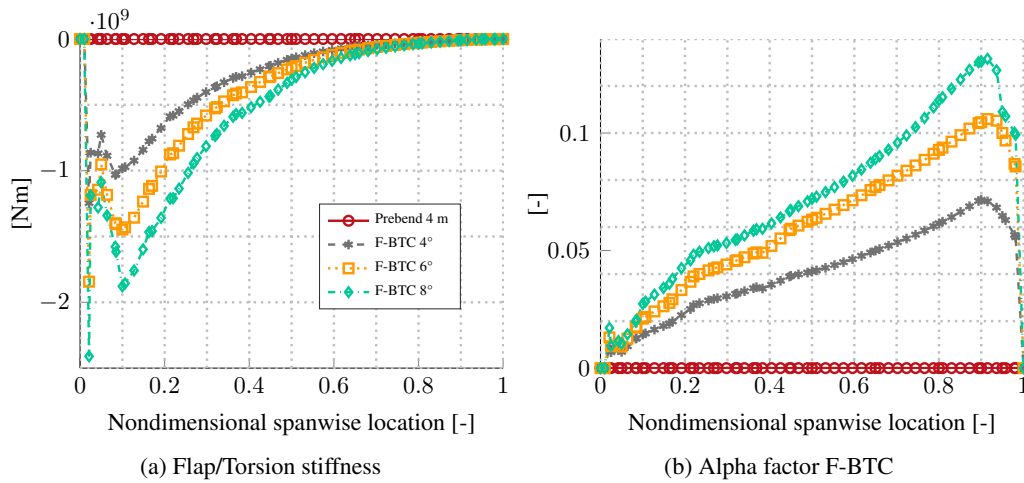


Figure 4.2.1: F-BTC blade coupling parameters.

4.2 Spar caps fiber rotation

In this step, the effects of the F-BTC passive control system will be explored. The technique consists of a rotation towards the leading edge of the spar cap fibers, with the intent to introduce a coupling effect between the out of plane deflection and the torsion of the blade. In particular, with a suitable rotation of the fibers, a flap-up bending implies a nose-down sectional rotation. Hence, depending on the magnitude of the coupling effect, when the blade deflects an automatic induced torsion is obtained at sectional level, which ultimately results in a reduction of the angle of attack and, due to the linearity of the $C_L - \alpha$ curve in the normal operating range of the wind turbine, in lower loads. An undesired consequence of the coupling mechanism is that, due to the larger torsional deformations, each section is driven away from its maximum efficiency conditions and works at a sub-optimal aerodynamic inflow. The overall consequence is that the loads and possibly the total blade mass can be significantly reduced, but some AEP is lost during turbulent simulations. Such conclusions have been demonstrated by dedicated studies which have been carried out in the last years. An in-depth analysis of the positive and negative aspects of the F-BTC is given for example in [11].

In this work a complete structural optimization loop for varying fiber orientation angles of 4°, 6° and 8° were respectively performed, in order to find which configuration ensures the best advantages in terms of load, blade mass, AEP and CoE. The effects of the fiber orientation on the blade characteristics can be summarized by the parameters illustrated in Figure 4.2.1. As shown, the introduction of a

Table 4.2: Mass, AEP and CoE comparison between F-BTC solutions and Prebend 4 m.

	Mass [kg]	AEP [GWh/yr]	CoE [\$/MWh]
Prebend 4 m	107446	91.80	82.44
F-BTC 4°	106464	91.75	82.51
F-BTC 6°	104810	91.63	82.58
F-BTC 8°	111780	91.61	82.61

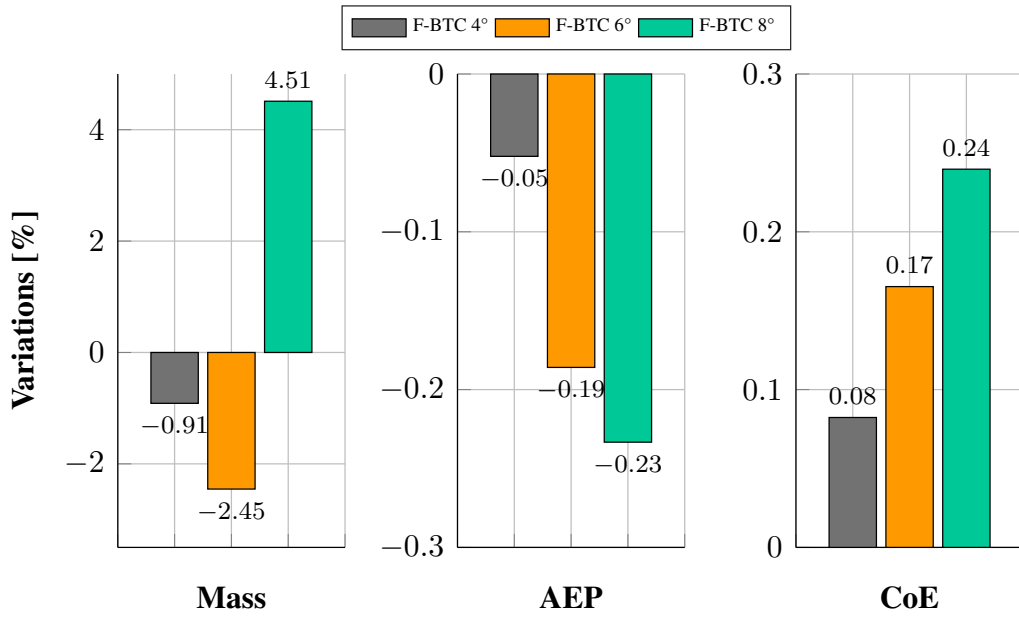


Figure 4.2.2: Performance percentage variation with respect to the 4 m Prebend model.

certain amount of F-BTC results in the appearance of a coupling term in the stiffness matrix. In particular, the extra-diagonal term which relates the out-of-plane and the torsional response of the blade is different from zero, and the magnitude of the coupling grows stronger as larger rotations are introduced in the fibers. The same trend can be evaluated in a different way by looking at the nondimensional coupling factor α_{FT} , which gives a measurement of the ratio between the extra-diagonal stiffness terms and the corresponding flap and torsional stiffness. A stronger coupling, then, is associated by a higher value of the coefficient as discussed in [11].

As expected, the AEP is lower for all the investigated solutions. Additionally, higher energy losses are experienced when the rotation of the fibers is larger. A

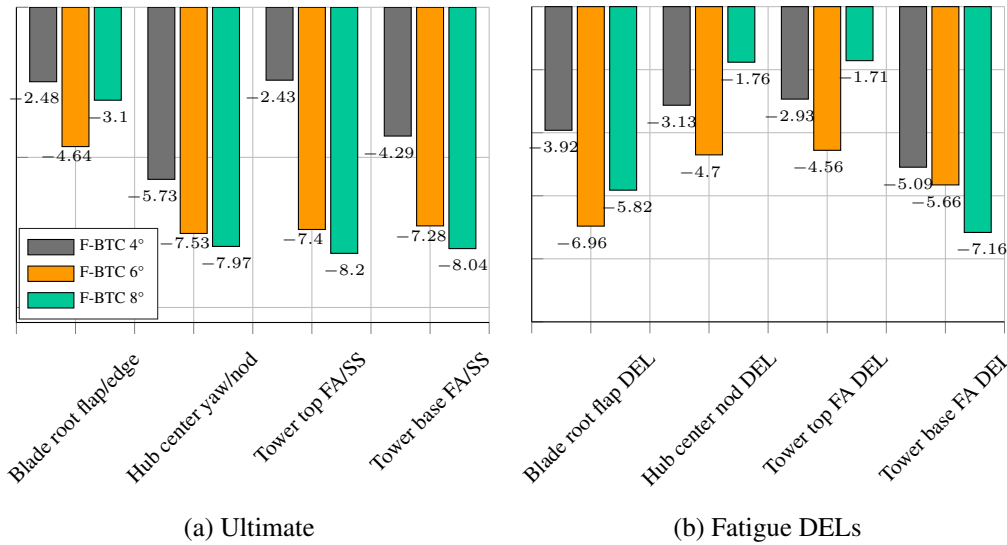


Figure 4.2.3: Key loads percentage variation with respect to the Prebend 4 m model.

blade mass gain is encountered in the first two cases, thanks to the loads mitigation and partial transfer from the bending moment to the torsional one. However, the mass saving is limited by the tip deflection constraint, which requires the loss in flapwise stiffness to be compensated by adding additional plies in the spar caps. Additionally, for larger fiber rotations these benefits are neutralized. In particular, as it can be deduced from Figure 4.2.4, fatigue phenomena on some blade elements due to the higher torsional and edgewise DELs loads drive the optimization to a globally heavier solution. From an economic perspective, the cost of energy worsen in all cases due to the AEP deterioration, and the limited mass saving can not fully counterbalance the impact.

The loads mitigation effects can be appreciated in Figure 4.2.3, where many of the key loads for both ultimate and fatigue cases results to be lower with respect to the initial configuration. The advantages of this passage are clearly related to a further redesign of other turbine components in which the F-BTC effect can play an important role.

Considering the overall aspect of the effects of F-BTC technology, the model with a 6° fibers rotation was taken as the one achieving significant mass and loads alleviation.

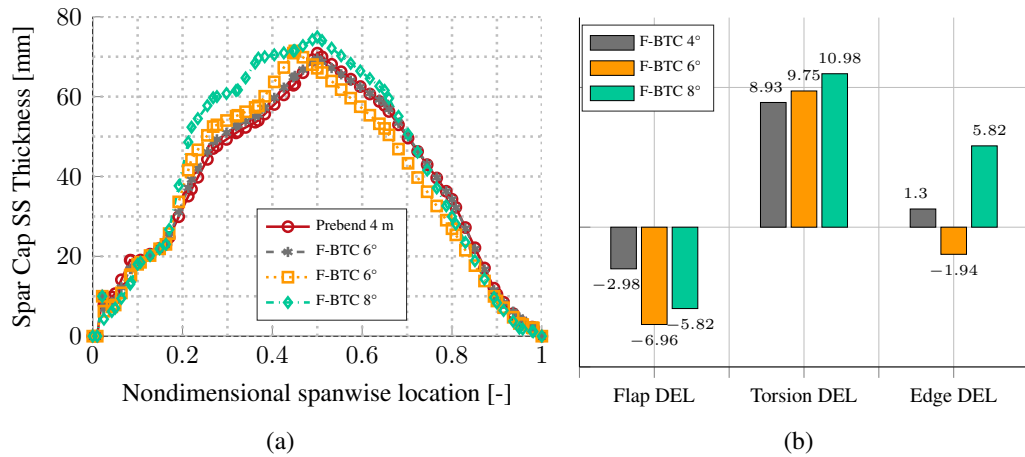


Figure 4.2.4: Suction side spar cap thickness (a) and blade root fatigue DELs (b) variations.

4.3 IPC

The next step was the introduction of another control system, based on an Individual Pitch Control (IPC) strategy. This is an active control, since it is based on the imposition of a pitch control input calculated on the basis of the recorded bending moments at the root of the blades. In particular such moments are transported in the fixed reference frame by means of a Coleman transformation that provides the tilt and yaw moments acting on the hub. Then, two independent control inputs, which aim is the reduction of the two moments, are computed by two separate PI controller still in the fixed frame. Finally, an inverse Coleman transformation is applied to the inputs and the resulting pitch control input is evaluated and superimposed to the signal calculated by the collective pitch and torque controller that continue to work on the machine in parallel with the new one. The described architecture is based on the one proposed by Bossanyi (2002) [8].

The IPC control is active both in normal operating conditions and during response to gusts, then it is expected to affect both ultimate and fatigue DELs loads. However, due to the nature of the transformation, the seconds are expected to be more influenced. The Coleman transformation in fact is based on frequency analysis aimed at splitting the harmonic frequencies that characterize the encountered loads. In particular tilt-yaw coupling phenomena identification and the relative frequency splitting is the main issue addressed by this control technique.

As happened for the F-BTC, the annual energy production should suffer a reduction due to the correction introduced in the pitch angle, as can be seen in Figure 4.3.1. It must be noticed how the new input signal act more rapidly with

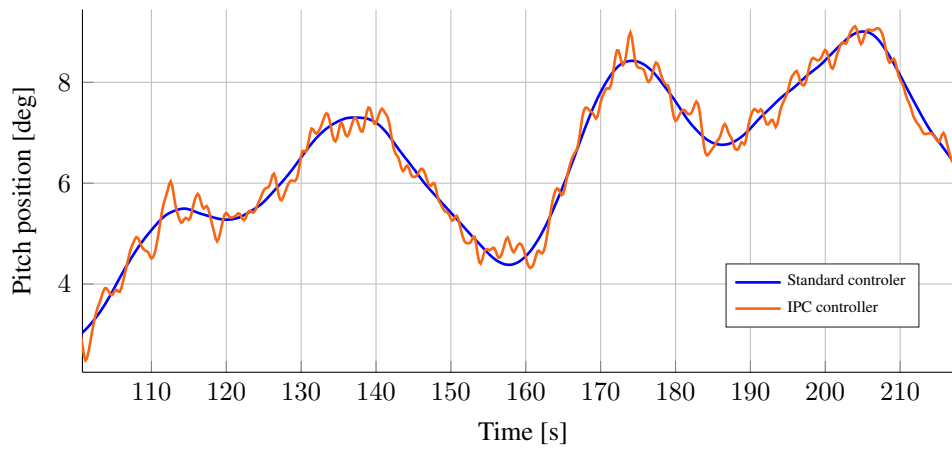


Figure 4.3.1: Time history of blade pitch angle with and without IPC during a 13 m/s operational condition. In the second case slightly faster and larger pitch movement are required in order to achieve the improved load reductions.

Table 4.3: Mass, AEP and CoE comparison between IPC solution and F-BTC 6° model.

	Mass [kg]	AEP [GWh/yr]	CoE [\$/MWh]
F-BTC 6°	104810	91.63	82.58
IPC	103141	91.39	82.71

respect to the collective signal, and problems of cumulative damage may occur in the actuators, however, this issue was not addressed in this work. The main advantages can be seen on loads variation, upon which the IPC is expected to act significantly. A reduction in important key loads is encountered, as can be seen in Figure 4.3.2, with particular effect on blade and tower roots fatigue DELs, and the hub ultimate loads. Figure 4.3.3 shows the resulting performances: a mass reduction derived by the lower loads occurred, while the AEP suffers a slight reduction as expected, which leads to a CoE worsening. Again, a complete redesign of the wind turbine is even more important in this case in order to completely capture the advantages found in loads reduction, especially on the tower, which gives an important contribution to the computation of the Initial Capital Cost (ICC), and thus to the CoE.

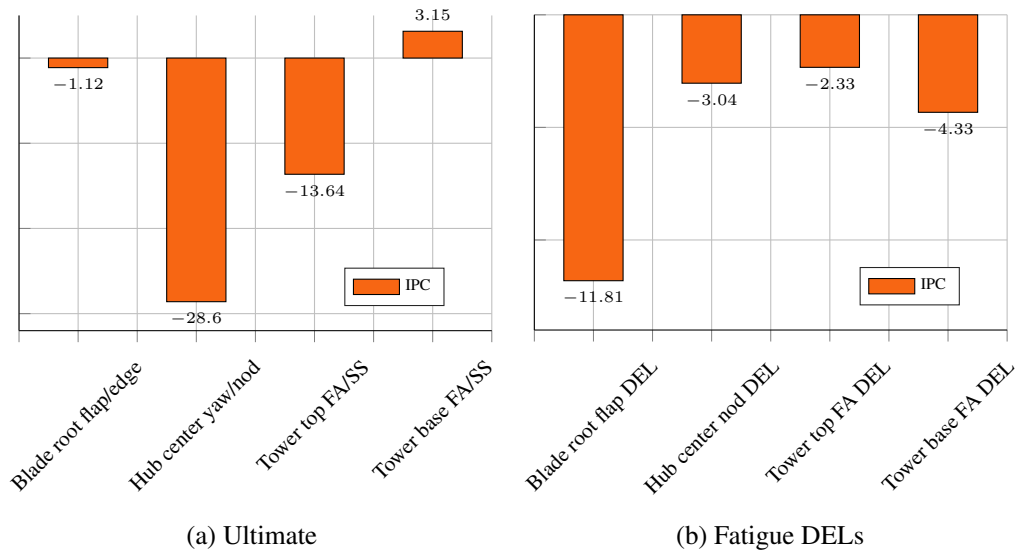


Figure 4.3.2: Key loads percentage variation with respect to the F-BTC 6° model.

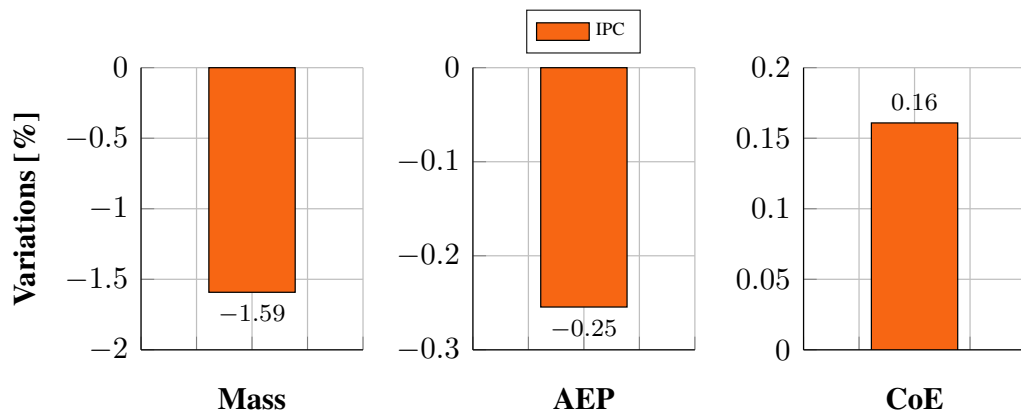


Figure 4.3.3: Performance percentage variation with respect to the F-BTC 6° model.

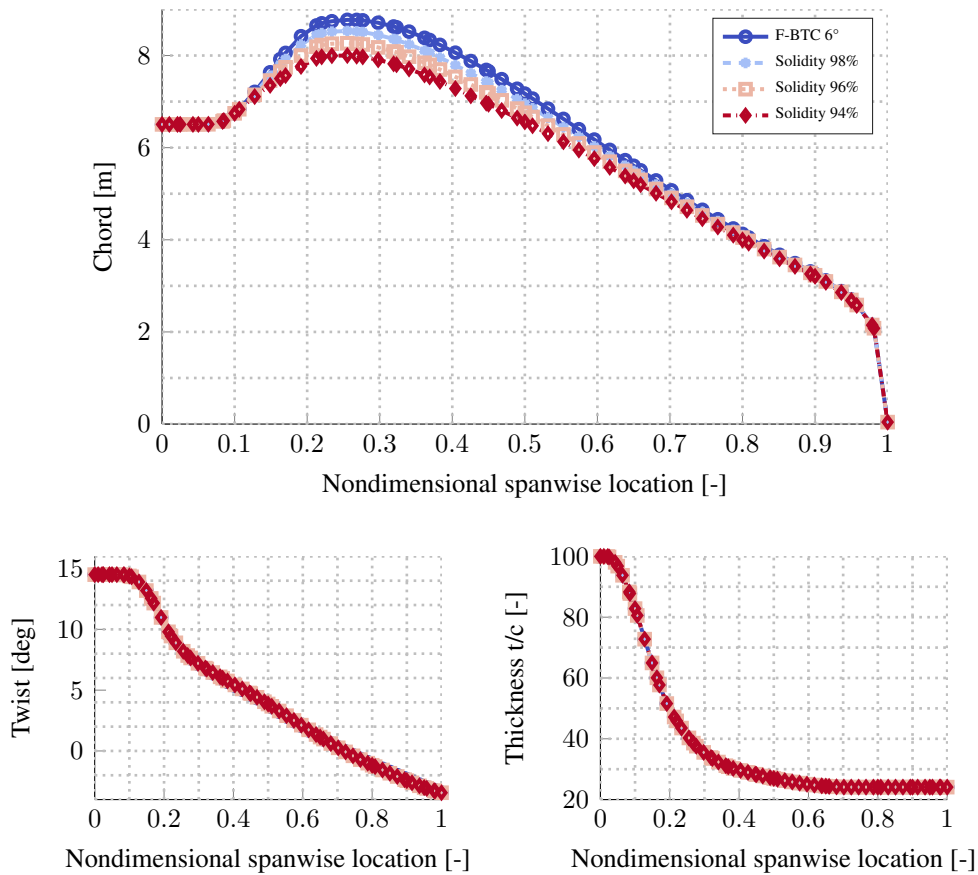


Figure 4.4.1: Chord, twist and relative thickness distribution variations.

4.4 Planar solidity

The last application in this work explores the planar solidity of the rotor. This figure represents the ratio between the portion of rotor area physically occupied by the blades and the total disk surface. It is an important parameter of the wind turbine, which impacts the aerodynamic efficiency of the wind turbine as well as the theoretical operating TSR. For example, for the same rotor size, a 2-blade turbine clearly has a lower planar solidity with respect to a 3-blade one. As a direct consequence, in the first case the achievable power coefficient happens to be lower, because only two blades instead of three contribute to the torque generation.

Starting from the optimal partial configurations identified in previous steps, cases in which the rotor solidity is reduced to 98%-96%-94% with respect to that of

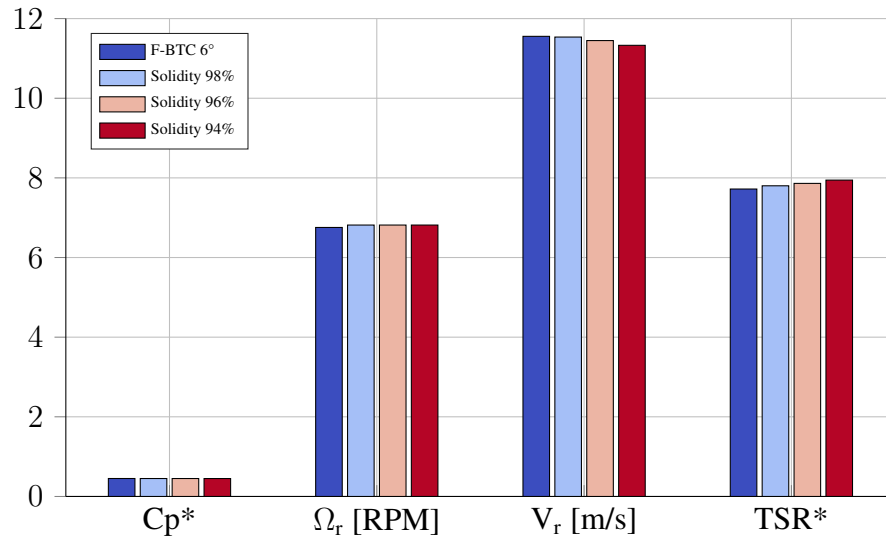


Figure 4.4.2: Rated conditions comparison.

the Baseline 20 MW, were investigated. In this case, the C_p -Max aerodynamic design module is employed ahead of the structural design so that AEP-maximizing distributions of chord, twist and nondimensional thickness can be identified for a certain value of the solidity. As mentioned in the description of the methods, the target value of the solidity is applied at Macro-level and acts as a constraint for the aerodynamic module. This means that the chord is optimized in a way that matches the target solidity. Also the twist and relative thickness distributions are allowed to change in order to maximize the AEP, but in these applications they are modified in a limited way as shown in Figure 4.4.1. Additional benefits could be obtained by considering more detailed study of the root region of the blade, which must be designed considering the necessary connection joints. The aim is to increase the annual power production by exploiting the fact that higher tip speed ratios can compensate the power detriment caused by the imposition of the minimum rotor speed. Furthermore, it must be considered that a solidity reduction leads to a lower maximum chord of the blade, which might result in advantages concerning lower manufacturing, transportation and installation costs. However, if the blade structure is heavily driven by stiffness requirements, for example because the tip displacement constraint is active, higher blade masses are expected for low-solidity design.

Theoretically, also a solidity increment could lead to higher AEP following the reverse reasoning, since lower TSR would be expected but higher rated power coefficients can be achieved. The huge value of the initial maximum chord is the main motivation behind the tentative approach to a solidity reduction.

Results agree with theoretical expectations in terms of rated conditions, as it can be seen in Figure 4.4.2. The optimal power coefficient suffers a small decrease while, as expected, the TSR increases. It must be noticed that due to the high operating TSR a $\Pi_{\frac{1}{2}}$ region appear which limits the rated rotor speed due to the maximum tip velocity limitation.

The AEP grows as expected in all the three cases, while the blade mass increases as the solidity is lowered. Both results agree with the expectations, in particular the mass increase which is related to the additional material which is required to compensate the lower sectional inertia originating from the lower blade surface and thickness. Globally, the AEP improvement cover the mass increment and a better CoE is achieved in all cases.

Table 4.4: Mass, AEP and CoE comparison between Solidity solutions and F-BTC 6° model.

	Mass [kg]	AEP [GWh/yr]	CoE [\$/MWh]
F-BTC 6°	104810	91.63	82.58
Solidity 98%	106584	91.72	82.45
Solidity 96%	107772	91.74	82.42
Solidity 94%	110229	91.73	82.43

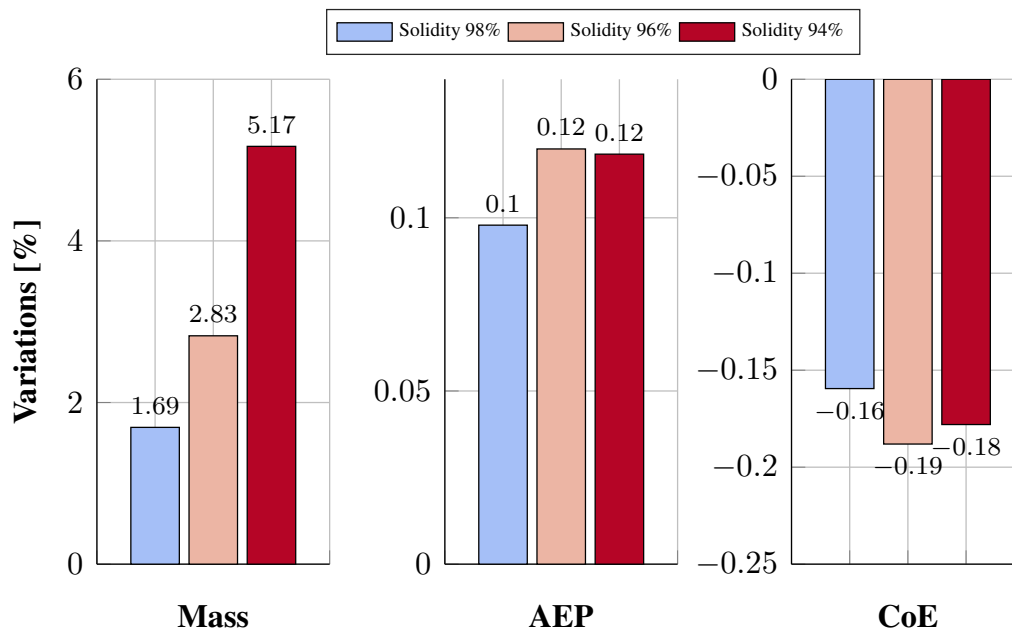


Figure 4.4.3: Performance percentage variation with respect to the F-BTC 6° model.

Positive effects are present also on the key loads for both ultimate and fatigue

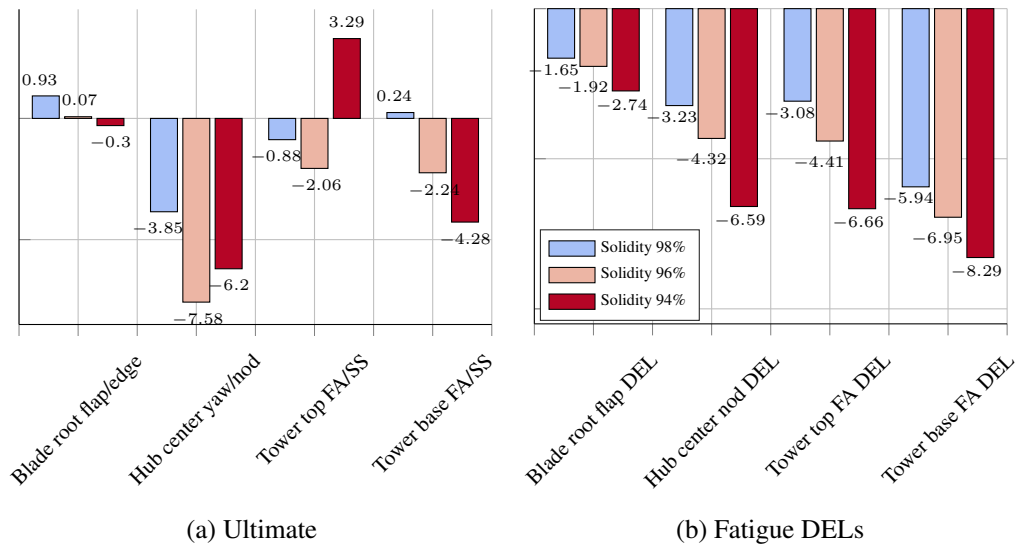


Figure 4.4.4: Key loads percentage variation with respect to the F-BTC 6° model.

cases, which may be related to the lower 'sail effect' associated to a reduced surface/wind interaction. Since the 96 % solidity allows the best CoE reduction, the solution is taken as the most promising and represents the best option identified at the end of the step-by-step parametric redesign.

4.5 Results

In Table 4.5 the main results of this work are summarized by comparing the Baseline 20 MW starting model with the achieved optimized solutions. It can be seen that in both cases remarkable loads and rotor mass reductions occur, according to the aim of this work. The mitigation effects are more relevant with the IPC control system, but the Solidity 96% solution can improve also the annual energy production, thus leading to an economical benefit in terms of cost of energy. A further step could ideally be done, by applying the IPC control system to the Solidity 96% model. This way it should be possible to combine the beneficial effects of both techniques.

Table 4.5: Solutions comparison

		Baseline 20 MW	IPC	Solidity 96%
Performance	Mass [kg]	113505	103141 (-9.13%)	107772 (-5.05%)
	AEP [GWh/yr]	91.62	91.39 (-0.25%)	91.74 (+0.13%)
	CoE [\$/MWh]	82.64	82.71 (+0.08%)	82.42 (-0.27%)
Ultimate loads	Blade root bending [MNm]	172.79	165.10 (-4.45%)	167.09 (-3.30%)
	Hub bending [MNm]	112.91	7.591 (-32.7%)	98.26 (-13.0%)
	Tower top bending [MNm]	105.29	90.38 (-14.2%)	102.50 (-2.65%)
	Tower base bending [MNm]	1480.42	1447.11 (-2.25%)	1371.52 (-7.36%)
Fatigue DELs	Blade root flap DEL [MNm]	84.38	68.00 (-19.4%)	75.63 (-10.4%)
	Hub nodding DEL [MNm]	54.75	47.32 (-13.6%)	46.69 (-14.7%)
	Tower top FA DEL [MNm]	54.89	47.78 (-12.9%)	46.77 (-14.8%)
	Tower base FA DEL [MNm]	288.48	279.25 (-3.20%)	271.61 (-5.85%)

CHAPTER 5

Conclusions

This work illustrates and discusses the results of the design for a conceptual 20 MW wind turbine rotor developed within the INNWIND.EU project. At first, a Reference 20 MW aero-elastic model was obtained by upscaling the 10 MW RWT. Then, its structural definition was used as a target for the design of the blade, which was performed by the structural module of the multi-disciplinary design algorithm $C_p\text{-Max}$. It was shown that the optimized structure provided characteristics in terms of blade stiffness, mass, and loads which are comparable to those of the Reference 20 MW. Since the resulting solution has a very high rotor mass, several optimization studies were performed in order to reduce mass and loads as much as possible. For each analysis, a full structural redesign was performed upon each solution, so that all the investigated configurations are designed according to the same goals and constraints. Variations of prebend distributions helped to achieve a higher AEP and provided room for a solid decrease of the rotor mass: this was obtained by taking advantage of the larger deflections allowed by the introduction of a certain prebend. Although a limited increment in the loads was detected, this was circumvented entirely by the application of passive and active control systems, which act on the ultimate and fatigue loads alleviation, laying the fundamentals for a positive redesign of the other wind turbine systems. They also allowed to design a lighter blade, albeit at the expenses of an acceptable

detriment of the AEP. Finally, a study on the rotor solidity shown that possible improvements in terms of AEP can be achieved, but with negative impacts on the blade mass. On the other side, the advantages obtained in the loads can lead to positive global improvements in the turbine re-design, which will definitely mitigate this leak.

Generally, it was found that mass and loads are heavily correlated to the investigated design features, and consequently they changed a lot according to the various design strategies involved. On the contrary the AEP and the cost of energy show only limited variations throughout this study, at least in terms of percent variations.

Moreover, looking in more details the Cost of Energy, it must be highlighted that its presented evaluations give only an overview of the economical aspects of the wind turbine. In fact, at a first glance the CoE value seems to be less attractive than the actual state of the art, represented by turbines with a lower rated power. However, even if the CoE model used in all the analyses represent the state-of-the-art, considerations about the benefits coming from the installation of less machines for the same capacity at a wind farm level have not been taken into account, albeit they could hid additional unexplored economical advantages. Again, many other technological, manufacturing and operational aspects have to be considered besides the load and mass alleviation, as preliminary done here. For example the higher manufacturing cost of a blade with a prebend distribution, or the waste of material due to the fiber rotation in the F-BTC technology have not been taken into account. A detailed cost model able to catch also these aspects should be developed in order to obtain a more realistic CoE evaluation that can be used as optimization driver in this kind of works, or as a benchmark between different wind turbine concept.

5.1 Future developments

The complexity of the problem and the high computational time required to achieve an optimal design solution with this high level of detail are the main limitations in suggesting a more detailed exploration of the design space during this work. However, the performed studies give an overview of how the analysed parameters impact on this type of turbine, and allow the definition of a good starting point for future works.

Some ideas for possible future developments are here proposed:

- Since many studies were performed during the optimization process, a de-

tailed analysis with a finite element method (FEM) was not performed at each step, but it should be carried out at least for the final optimal solution in order to verify the rotor integrity and the fulfilment of all desired structural constraints (e.g. allowables, fatigue, buckling). Such requirements are already considered in the followed structural design process and therefore small variations with respect to the present model are expected due to the higher level of detail. The C_p -Max environment allows the automatic definition of a detailed FEM model of the blade that can be directly run in NASTRAN to capture the three-dimensional state of stress and strain with a high level of precision. Static, modal and fatigue analyses are performed at this scope, using loads computed at the aero-elastic level, and results are used to update data and bounds for the next iteration of the optimization loop.

- As anticipated, other passive control systems can be added to the present configuration to further improve mass and loads alleviation. First of all, the F-BTC technology adopted for the spar caps fibers can be extended also to others blade structural elements such as the shell panels. Another example is the offset-induced BTC (O-BTC), which is based on a geometrical misalignment of the spar caps planar positions, which ultimately generates a coupling between the out-of-plane and in-plane response of the blade. Additional coupling could be obtained through the sweep-induced (S-BTC) coupling, in which an in-plane curvature of the pitch axis is introduced which results in a swept planform for the blade. A possible way to follow is also to combine the various technologies together in order to find out potential synergies that counteract negative aspects of each feature. Alternatively, improvements from active control system can be achieved for example with flaps and movable tips. In these cases, disadvantages would emerge from higher manufacturing, operative and maintenance costs should be considered.
- Study some way to improve the annual energy production is also a must. In particular, detriment caused by the imposition of a rotation speed lower bound could be easily overcome by a dedicated optimization of the scheduled pitch angle at low wind speeds. Another possible strategy to limit the AEP losses in F-BTC solutions could rely on a wind-varying pitch schedule for the partial-load operating range. In this view, instead of prescribing a single pitch value for the whole range below the rated speed, one could think of prescribing multiple values for various wind speed, so that different level of torsion can be optimally compensated. The result should be beneficial in terms of net AEP, although impacts on the Actuator Duty Cycle

(ADC) should be expected.

- Other wind turbine components should be re-designed, taking advantage from the results obtained in the rotor design in term of loads reduction. In particular, the tower has an important impact on the CoE in terms of initial capital cost. Thus, its optimization could lead to an important mass and costs reduction if conducted considering also the possible mass reductions for the overall top tower elements (blade, nacelle and hub). $C_p\text{-Max}$ can handle this task, as illustrated in Chapter 3, allowing at the same time the verification of all the constraints required for achieving a meaningful solution.
- As mentioned, the approach employed in this work relies on a step-by-step optimization of selected features of the turbine. Although significant advantages have been obtained, it would be interesting to perform a redesign in a fully automatic way, that is, by exploiting the Macro-design capabilities of $C_p\text{-Max}$. Although being complex and computationally expensive, the latter (monolithic) approach ensures a true and continuous exploration of the design space, in a classical sense, whereas in this study some parameters like the maximum prebend or the fiber angle were manually changed during the various design steps. It would be very interest to know if the results of a fully-automated design process would confirm or contradict the conclusions of this work.

APPENDIX A

Controller data

Table A.1: Settings of the DTU Controller.

Parameter	Value	Descriptor
Overall parameters		
P0	21276.6	Rated power [kW]
Omega_min	0.4398	Minimum rotor speed [rad/s]
Omega_0	0.6594	Rated rotor speed [rad/s]
GenTorque_max	4.04E+07	Maximum allowable generator torque [Nm]
Theta_min	100	Minimum pitch angle (if 100 → wpdata)
Theta_max	90	Maximum pitch angle [deg]
ThetaDot_max	7.071	Maximum pitch velocity operation [deg/s]
omega_Omega	0.14	Frequency of generator speed filter [Hz]
Zeta_Omega	0.7	Damping ratio of speed filter [-]
omega_n	2.35	Frequency of free-free DT torsion mode [Hz], if zero no notch filter used
Partial load control parameters		
K	5.137E+07	Optimal Cp tracking K factor [kNm/(rad/s) ²]
kg_P	2.73E+08	Proportional gain of torque controller [Nm/(rad/s)]
kg_I	4.34E+07	Integral gain of torque controller [Nm/rad]
kg_D	0	Differential gain of torque controller [Nm/(rad/s ²)]
Full load control parameters		
GenControlStrategy	2	Generator control switch [1=constant power, 2=constant torque]
k_P	0.524	Proportional gain of pitch controller [rad/(rad/s)]
k_I	0.099	Integral gain of pitch controller [rad/rad]
k_D	0	Differential gain of pitch controller [rad/(rad/s ²)]
kP_P	2.00E-09	Proportional power error gain [rad/W]
kP_I	1.41E-09	Integral power error gain [rad/(Ws)]
K_1	198	Coefficient of linear term in aerodynamic gain scheduling, KK1 [deg]
K_2	693	Coefficient of quadratic term in aerodynamic gain scheduling, KK2 [deg ²]
Omega_2OnOmega_0	1.3	Relative speed for double nonlinear gain
Cut-in simulation parameters		
CutInTime	0	Cut-in time [s]
CutInDelay	5.65	Time delay for soft start of torque [1/1P]
Cut-out simulation parameters		
Tau_out	0	Cut-out time [s]
TTorqueFilter	3.53	Time constant for 1st order filter lag of torque cut-out [s]
StopType	1	Stop type [1=linear two pitch speed stop, 2=exponential pitch speed stop]
TimeDelayPitchStop1	1.41	Time delay for pitch stop 1 [s]
ThetaDot_max_Stop1	14.14	Maximum pitch velocity during stop 1 [deg/s]
TimeDelayPitchStop2	1.41	Time delay for pitch stop 2 [s]
ThetaDot_max_Stop2	7.071	Maximum pitch velocity during stop 2 [deg/s]

Table A.1: (Continued)

Expert parameters		
Theta_f_0	0.5	Lower angle above lowest minimum pitch angle for switch [deg]
Theta_f_1	0.5	Upper angle above lowest minimum pitch angle for switch [deg]
gamma	95.0	Percentage of the rated speed when the torque limits are fully opened
Tau_V_Omega0	7.0711	Time constant of 1st order filter on wind speed used for minimum pitch [1/1P]
Tau_Theta_Omega0	7.0711	Time constant of 1st order filter on pitch angle for gain scheduling [1/1P]
Drivetrain damper		
k_dmp	1.8e7	Proportional gain of DT damper [Nm/(rad/s)], requires frequency in input 10
Over speed shutdown		
OverspeedPercentage	1500	Over speed percentage [%], before initiating shut down
Additional non-linear pitch control term		
Omega_os	0.0	Rotor speed error scaling factor [rad/s]
OmegaDot_os	0.0	Rotor acceleration error scaling factor [rad/s ²]
k_os	0.0	Pitch rate gain [rad/s]

Bibliography

- [1] Ashuri T., and Zaaijer M.B. *Size effect on wind turbine blades design driver*. In European Wind Energy Conference and Exhibition, Brussels, Belgium, pages 1-6. European Academy of Wind Energy, 2008.
- [2] Ashuri T. *Beyond classical upscaling: integrated aeroservoelastic design and optimization of large offshore wind turbines*. Ph.D. thesis. the Netherlands: Delft University of Technology, 2012.
- [3] Ashuri T., Zaaijer M.B., Martins J.R.R.A., van Bussel G.J.W., van Kuik G.A.M. *Multidisciplinary design optimization of offshore wind turbines for minimum levelized cost of energy*. *Renew. Energ.*, 68, 893-905 doi:10.1016/j.renene.2014.02.045, 2014.
- [4] Ashuri T., Zaaijer M.B., Martins J. R.R.A., and Zhang J. *Multidisciplinary design optimization of large wind turbines - Technical, economic, and design challenges*. *Energy Conversion and Management* 123, 56-70, 2016.
- [5] Bak C., Zahle F., Bitsche R., Kim T., Yde A., Henriksen L.C., Andersen P.B., Natarajan A., and Hansen M.H. *Description of the DTU 10 MW reference wind turbine*. DTU Wind Energy Report-I-0092, July, 2013.
- [6] Björk, A. *Coordinates and Calculations for the FFA-W1-xxx, FFA-W2-xxx and FFA-W3-xxx Series of Airfoils for Horizontal Axis Wind Turbines*. FFA TN 1990-15, Stockholm, Sweden, 1990.

- [7] Bortolotti P., Bottasso C.L., and Croce A. *Combined preliminary-detailed design of wind turbines*. Wind Energ. Sci., 1, 71-88, 2016.
- [8] Bossanyi E. *Individual Blade Pitch Control for Load Reduction*. Wind Energ., 6, 119-128, doi: 10.1002/we.76, 2002.
- [9] Bottasso C.L., Croce A. *Cp-Lambda a Code for Performance, Loads, Aeroelasticity by Multi-Body Dynamics Analysis*. Ver. 5.20, Politecnico di Milano, 2010-2017.
- [10] Bottasso C.L., Croce A., Campagnolo F. *Multi-disciplinary constrained optimization of wind turbines*. Multibody Syst. Dyn., 27, 21-53, 2012.
- [11] Bottasso C.L., Campagnolo F., Croce A., Tibaldi C. *Optimization-based study of bend-twist coupled rotor blades for passive and integrated passive/active load alleviation*. Wind Energ., 16, 1149-1166, doi:10.1002/we.1543, 2013.
- [12] Bottasso C.L., Campagnolo F., Croce A., Dilli S., Gualdoni F., and Nielsen M.B. *Structural optimization of wind turbine rotor blades by multi-level sectional/multibody/3-D-FEM analysis*. Multibody Syst. Dyn., 32, 87-116, doi:10.1007/s11044-013-9394-3, 2014.
- [13] Buckney N., Pirrera A., Weaver P., Griffith D.T. *Structural efficiency analysis of the sandia 100 m wind turbine blade*. AIAA Science and Technology Forum and Exposition 2014: 32nd ASME Wind Energy Symposium, National Harbor, 2014.
- [14] Capponi P.A.C., Ashuri T., van Bussel G.J.W., and Kallesøe B. *A non-linear upscaling approach for wind turbine blades based on stresses*. In European Wind Energy Conference and Exhibition, Brussels, Belgium, pages 1-8. European Academy of Wind Energy, 2011.
- [15] Chaviaropoulos P. *Similarity rules for wind turbine upscaling*. Internal report, UPWIND, 2007.
- [16] Chaviaropoulos P., and Milidis A. (NTUA). *20 MW Reference Wind Turbine Aeroelastic data of the onshore version*. Internal report, INNWIND.EU, 2011.
- [17] Cox K., Echtermeyer A. *Geometric Scaling Effects of Bend-twist Coupling in Rotor Blades*. Energy Procedia, 35, 2-11, doi:10.1016/j.egypro.2013.07.153, 2013.
- [18] Croce A., Sartori L., Lunghini M.S., Clozza L., Bortolotti P., Bottasso C.L. *Lightweight rotor design by optimal spar cap offset*. J. Phys.: Conf. Ser., 753, 2016.

- [19] DNV GL *Bladed wind turbine simulation tool*. URL:<https://www.dnvgl.com/services/bladed-3775>
- [20] Fingersh L., Hand M., and Laxson A. *Wind turbine design cost and scaling model*. Technical Report NREL/TP-500-40566, 2006.
- [21] Giavotto V., Borri M., Mantegazza P., Ghiringhelli G. *Anisotropic beam theory and applications Comput. Struct.*, 16, 403-13, 1983.
- [22] Griffith D.T., Johanns W. *Large blade manufacturing cost studies using the Sandia blade manufacturing cost tool and Sandia 100-meter blades*. SANDIA Report SAND2013-2374, SANDIA National Laboratories, Albuquerque, USA, 2013.
- [23] Germanischer Lloyd. *Guideline for the Certification of Wind Turbines*. Hamburg, Germany, 2010.
- [24] Hansen M.H., Henriksen L. C. *Basic DTU Wind Energy controller*. DTU Wind Energy, Technical University of Denmark, 2013.
- [25] INNWIND.EU *Deliverable 1.23, PI-based assessment of innovative concepts (methodology)*. INNWIND.EU technical report, Deliverable 1.23, available at: www.innwind.eu, April 2014.
- [26] International Electrotechnical Commission. *IEC 61400-1 Wind Turbines - Part 1: Design Requirements*, 3rd Edition, 2006.
- [27] Jamieson P. *Innovation in Wind Turbine Design*. Wiley, 2011.
- [28] Jamieson P. *Loading and cost trends using certification calculation*. Internal report, UPWIND, 2007.
- [29] Jonkman B.J. and Kilcher L. *TurbSim User's Guide: Version 1.06.00*. NREL Technical Report, September 2012.
- [30] Lobitz D.W., Veers P.S. *Aeroelastic behavior of twist-coupled HAWT blades*. AIAA-98-0029 doi:10.2514/6.1998-29, 1998.
- [31] Lobitz D.W., Veers P.S. *Load Mitigation with Bending/Twist-coupled Blades on Rotor Using Modern Control Strategies*. *Wind Energ.*, 6, 105-117, doi:10.1002/we.74, 2003.
- [32] Management Knowledge Centre WMC *FOCUS6: The integrated Modular Wind Turbine Design Suite*. URL:[https://www.wmc.eu/pdf/WMC focus6 2017.pdf](https://www.wmc.eu/pdf/WMC_focus6_2017.pdf)

- [33] Molly J. *Maximum economic size of wind energy converters*. European Wind Energy Conference, 1989.
- [34] NASA Glenn Research Center *Multidisciplinary Design Analysis and Optimization (MDAO)*. URL:<http://openmdao.org/>.
- [35] National Renewable Energy Laboratory (NREL) *Framework for Unified Systems Engineering and Design of Wind-Plants (FUSED-Wind)*. URL:<https://nwtc.nrel.gov/Integrated-System-Tools>.
- [36] Nijssen R., Zaaijer M., Bierbooms W., van Kuik G., and van Delft D. *The application of scaling rules in up-scaling and marinisation of a wind turbine*. Offshore Wind Energy Special Topic Conference, 2001.
- [37] Ning A., Damiani R., Moriarty P. *Objectives and constraints for wind turbine optimization*. 51st AIAA Aerospace Sciences Meeting, Grapevine, USA, January 7-10, 2013.
- [38] Riboldi C.E.D. *Advanced control laws for variable-speed wind turbines and supporting enabling technologies*, Ph.D. Thesis, Politecnico di Milano, Milan-Italy, 2012.
- [39] Sartori L., Bortolotti P., Croce A., Bottasso C.L. *Integration of prebend optimization in a holistic wind turbine design tool*. TORQUE, Munich, Germany, 5-7 October, 2016.
- [40] Stäblein A.R., Hansen M.H. *Effect of Turbulence on Power for Bend-Twist Coupled blades*. J. Phys.: Conf. Ser.: 753 doi:10.1088/17426596/753/4/042018, 2016.
- [41] Vesel Jr. R.W., Mc Namara J.J. *Performance enhancement and load reduction of a 5 MW wind turbine blade*. Renew. Ener.g, 66, 391-401, doi: 10.1016/j.renene.2013.12.019, 2014.
- [42] Zahle F., Tibaldi C., Verelst D.R., Bak C., Bitche R., Blasques J.P.A.A. *Aero-Elastic Optimization of a 10 MW Wind Turbine*. AIAA SciTech 2015, Kissimmee, USA, January 5-9, 2015.